Joana Pinheiro Pimenta
Licenciada em Bioquímica

Peroxiporins Involvement in Oxidative Stress and their Potential for Drug Targeting

Dissertação para obtenção do Grau de Mestre em
Bioquímica para a Saúde

Orientadora: Prof. Drª Graça Soveral, Professora Catedrática, Faculdade de Farmácia, Universidade de Lisboa

Outubro 2022

Joana Pinheiro Pimenta
Licenciada em Bioquímica

Peroxiporins Involvement in Oxidative Stress and their Potential for Drug Targeting

Dissertação para obtenção do Grau de Mestre em
Bioquímica para a Saúde

Orientadora: Prof. Drª Graça Soveral, Professora Catedrática, Faculdade de Farmácia, Universidade de Lisboa

Júri:
Presidente: Prof. Drª Maria Teresa Nunes Mangas Catarino
Arguente: Drª Maria Manuela Gaspar
Vogal: Prof. Drª Graça Soveral

Faculdade de Ciências e Tecnologia da Universidade Nova de Lisboa

Outubro 2022

Peroxiporins Involvement in Oxidative Stress and their Potential for Drug Targeting

Peroxiporins Involvement in Oxidative Stress and their Potential for Drug Targeting

Joana Pimenta

2022

Peroxiporins Involvement in Oxidative Stress and their Potential for Drug Targeting

Peroxiporins Involvement in Oxidative Stress and their Potential for Drug Targeting

Peroxiporins Involvement in Oxidative Stress and their Potential for Drug Targeting

De acordo com o disposto no artigo 24º do Regulamento de Estudos de Pós-Graduação da Universidade de Lisboa, Despacho nº 7024/2017, publicado no Diário da República – 2ª Série – nº 155 – 11 de Agosto de 2017, foi utilizada nesta dissertação informação incluída nas seguintes publicações:

Apresentação Oral em Conferência Internacional:

da Silva I. V., **Pimenta, J.**, Silva, A. G., Casini, A., Soveral, G. (2022) Targeting AQP3 inhibits hydrogen peroxide and glycerol permeability and impairs cell proliferation and migration in melanoma. Aquaporin Meeting, Copenhagen (Denmark)

Poster em Conferência Nacional:

Pimenta, J., da Silva I. V., Silva, A. G., Casini, A., Soveral, G. (2022) Targeting AQP3 inhibits hydrogen peroxide and glycerol permeability and impairs cell proliferation and migration in melanoma. 13th iMed-ULisba Postgraduate Students Meeting, Lisbon (Portugal)

Poster em Conferência Internacional:

Pimenta, J., da Silva I. V., Silva, A. G., Casini, A., Soveral, G. (2022) Targeting peroxiporin AQP3 impairs hydrogen peroxide diffusion and cell proliferation in melanoma. The Biochemistry Global Summit – the 25th IUBMB, 46th FEBS and 15th PABMB Congresses, Lisbon (Portugal)

Acknowledgments

Agora que cheguei ao fim de mais uma etapa da minha vida, gostaria muito de agradecer a várias pessoas que foram cruciais neste último ano.

Em primeiro lugar, gostaria de agradecer à Professora Graça Soveral por me ter recebido no seu laboratório e por me dar a oportunidade de estudar um tema que eu gostei bastante. Para além disso, não tenho palavras para agradecer pela oportunidade de poder ter participado no Congresso da FEBS em Lisboa para apresentar os resultados que obtive. Foi muito bom poder ter tido a oportunidade de ter assistido a todas as palestras e ter podido interagir com pessoas de diferentes áreas e países.

De seguida, não podia deixar de agradecer à Inês e à Catarina. Aprendi muito com a Inês que fez um excelente trabalho a orientar o meu trabalho no laboratório e a tirar todas as dúvidas que eu tive tanto durante o trabalho prático como na análise dos meus resultados. Catarina, muito obrigada também por me ajudares sempre que era preciso e por me orientares naqueles três dias de Western Blot.

Gostava também de agradecer à Inês e Elisabete, as minhas duas colegas de mestrado e laboratório durante o ano de tese. Foram um grande apoio e companhia diária no laboratório.

Um obrigado também à minha irmã Mariana que mesmo estando longe me apoiou diariamente e que pelas nossas conversas fazia com que as duas horas de viagem de casa para a faculdade e vice-versa parecessem mais curtas.

Finalmente, o agradecimento mais importante. Quero muito agradecer à minha família que não me deixou desistir mesmo quando eu duvidava de mim mesma.

Peroxiporins Involvement in Oxidative Stress and their Potential for Drug Targeting

Resumo

As aquaporinas (AQP) peroxiporinas são canais transmembranares que facilitam a permeação de H_2O_2 através da membrana plasmática. Em concentrações elevadas, o H_2O_2 desencadeia stress oxidativo. Uma vez que a peroxiporina AQP3 se encontra sobreexpressa em vários cancros, como o melanoma, é um importante interveniente na biologia do cancro.

Neste estudo usaram-se células MNT-1 e A375 como modelo de melanoma. Primeiro, analisou-se a expressão do mRNA (qPCR) e proteína (Western Blot) da AQP3. Posteriormente, avaliou-se o efeito do Auphen, inibidor da AQP3, e de uma nova serie de compostos de ouro ($C^{CO}N$, $C^{NH}N$ e $C^{CH2}N$) na permeabilidade membranar à água, glicerol e H_2O_2 (microscopia de epifluorescência). O efeito dos compostos foi ainda avaliado por estudos de toxicidade, adesão, proliferação celular (ensaio colorimétrico de MTT), migração (fecho de ferida) e indução da apoptose (libertação de LDH).

Os resultados revelaram que a AQP3 é a AQP da membrana plasmática mais expressa nas linhas de melanoma. As células MNT-1 expressam mais mRNA, contudo, as A375 produzem mais proteína AQP3. O ensaio de toxicidade demonstrou que a concentração de composto que não compromete a viabilidade celular é 5 μM, sendo esta a concentração usada em ensaios subsequentes. Todos os compostos inibiram o transporte de glicerol via AQP3, sendo que $C^{CO}N$ (MNT-1) e $C^{CH2}N$ (A375) se mostraram mais potentes. O $C^{CO}N$ mostrou ser o melhor inibidor do transporte de H_2O_2. Por outro lado, o $C^{CH2}N$ reduziu mais a adesão celular. No caso das A375, o $C^{NH}N$ pareceu influenciar a redução da proliferação e migração celular. A proliferação das MNT-1 foi mais comprometida pelo $C^{CH2}N$ e a migração pelo $C^{CO}N$. O ensaio de LDH demonstrou que estes compostos não afetam a integridade membranar destas células.

Concluindo, a nova série de inibidores da AQP3 mostrou-se promissora e esta inibição parece afetar a progressão do melanoma, confirmando a AQP3 como um alvo promissor para terapias contra o cancro.

Termos chave: aquaporinas, peroxiporinas, permeabilidade, inibidores, melanoma

Peroxiporins Involvement in Oxidative Stress and their Potential for Drug Targeting

Abstract

The aquaporins (AQP) named peroxiporins are transmembrane channels that facilitate the permeation of H_2O_2 across biological membranes. At high concentrations, H_2O_2 triggers oxidative stress. Since AQP3 is found overexpressed in several cancers, such as melanoma, it may have an important role in the biology of cancer.

In this study, MNT-1 and A375 cells were used as melanoma cell models. First, the expression of AQP3 mRNA (qPCR) and protein (Western Blot) was analysed. Subsequently, the effect of Auphen, an AQP3 inhibitor, and a new series of gold compounds ($C^{CO}N$, $C^{NH}N$ and $C^{CH2}N$) was evaluated on membrane permeability to water, glycerol and H_2O_2. These compounds were further evaluated for their toxicity and effect on cell adhesion, proliferation (MTT colorimetric assay), migration (wound closure) and apoptosis induction (LDH release).

The results revealed that AQP3 is the most expressed plasma membrane AQP in melanoma lines. MNT-1 cells express more AQP3 mRNA, however, A375 cells produce more AQP3 protein. The toxicity test demonstrated that the concentration of compound that does not compromise cell viability is 5 μM, which was used for further experiments. All compounds inhibited glycerol transport via AQP3 with $C^{CO}N$ (MNT-1) and $C^{CH2}N$ (A375) being more potent. $C^{CO}N$ proved to be the best inhibitor of H_2O_2 transport. On the other hand, $C^{CH2}N$ reduce adherence the most. In the case of A375, $C^{NH}N$ appeared to influence the reduction of cell proliferation and migration. The proliferation of MNT-1 was more compromised by $C^{CH2}N$ and migration by $C^{CO}N$. The LDH assay demonstrated that these compounds do not affect the membrane integrity of these cells.

Overall, our data reveal that the impairment of H_2O_2 and glycerol permeability via AQP3 can affect melanoma skin cancer progression, unveiling AQP3 a promising drug target for cancer therapies. In addition, this new series of gold compounds revealed good candidates for cancer treatment since they decrease melanoma cell proliferation and migration.

Keywords: aquaporins peroxiporins, permeability, inhibitors, melanoma

Table of Contents

Figure index

Table index

Equation index

List of abbreviations

AKT - Protein kinase B

AQP(s) - Aquaporin(s)

Arg - Arginine

ar/R SF - Aromatic/arginine selectivity filter

Asn - Asparagine

ATP - Adenosine triphosphate

Auphen - $[Au(phen)Cl_2]Cl$

BSA - Bovine serum albumin

Calcein-AM - calcein-acetoxymethylester

CHIP28 - Channel-like integral protein of 28 kDa

Cys - Cysteine

E_a - Activation energy ($J.mol^{-1}$)

E-cadherin - Epithelial cadherin

ECM - Extracellular matrix

EGF - Epidermal growth factor

EGFR - Epidermal growth factor receptor

EM - Electron microscopy

EMT - Epithelial-mesenchymal transition

F - Fluorescence signals

GlpF - Glycerol facilitator from *Escherichia Coli*

HGF - Hepatocyte-derived growth factor

HIF-1α – Hypoxia-inducible factor 1-alpha

HIF-2α - Hypoxia-inducible factor 2-alpha

His - Histidine

Keap1 - Kelch-like ECH-associated protein 1

KO - Knockout

LDH - Lactate Dehydrogenase

MIP - Major intrinsic protein

MMPs - Matrix metallopeptidases

NF-κB – Nuclear factor kappa B

NIPS - Nodulin26-like proteins

NMO - Neuromyelitis optica

Nox – NADPH oxidase

NPA - Asparagine-proline-alanine

NPC - Asparagine-proline-cysteine

NPT - Asparagine-proline-threonine

Nrf2 - Nuclear factor-erythroid factor 2-related factor 2

PDGF - Platelet-derived growth factor

P_f - Water permeability coefficient

PG - Phosphatidylglycerol

P_{gly} - Glycerol permeability coefficient

Phe - Phenylalanine

PIPS - Plasma membrane intrinsic proteins

PLD_2 - Phospholipase D2

PTPs - Protein tyrosine phosphatases

RBCs - Red blood cells

RIPA - Radioimmunoprecipitation assay

ROS - Reactive oxygen species

RT-qPCR - Reverse-transcription quantitative PCR

SB - Stratum Basale

SC - Stratum Corneum

SG - Stratum Granulosum

SIPS - Small basic intrinsic proteins

SS - Stratum Spinosum

TGF-β - Transforming growth factor beta

TIPS - Tonoplast intrinsic proteins

VEGF - vascular endothelial growth factor

XIPS - Uncharacterized intrinsic proteins

1 Introduction

1.1 Aquaporins discovery and role in water homeostasis

Water is the main component of cells and tissues implying that water homeostasis is crucial for the cell's physiology [1,2]. To regulate homeostasis, water can cross cell lipidic bilayers by two different mechanisms of permeation: diffusion directly across the hydrophobic membrane (simple diffusion) and through channels that facilitate water diffusion (facilitated diffusion), named aquaporins (AQPs) [3]. Transport by aquaporin-mediated diffusion requires a lower activation energy (E_a) when compared to simple diffusion across cell membranes, ensuring the fast equilibration of osmotic gradients [2,3].

The first water channel was described in the membrane of erythrocytes and renal tubules [1]. This protein was originally designated as Channel-like integral protein of 28 kDa (CHIP28). The analysis of the CHIP28's amino acid sequence showed a common homology with the major intrinsic protein (MIP) from bovine lens cells. This reveals that the referred water channel is part of the MIP family of transmembrane channel proteins [4]. The water channel activity of CHIP28 was stablished by several experiments such as its the insertion in liposomes and the injection of the complementary RNA into *Xenopus laevis* oocytes [1,4]. In 2003, Peter Agre was awarded with the Chemistry Nobel Prize by his work in identifying and characterizing CHIP28 that was renamed aquaporin-1 (AQP1) [4].

1.2 Aquaporin family

AQPs are a family of transmembrane proteins whose main function is the passive and bidirectional transport of water and several other small molecules (such as glycerol, hydrogen peroxide, urea, and ammonia), through the plasma membranes in response to osmotic or solute gradients [4,5]. The AQP family is a highly conserved group of channel proteins composed of more than 1700 integral membrane proteins and found in all living organisms [3], belonging to the Major Intrinsic Protein (MIP) family.

In mammalian cells, AQPs are broadly distributed with specific organ, tissue, cellular and subcellular localizations [4,7]. AQPs can be found in organs and tissues related to fluid absorption and excretion but also in tissues that are not involved in the transport of fluids like brain, skin, fat and liver [3]. So far, 15 classes of aquaporin genes have been identified in mammals (AQP0-AQP14) [1].The first 13 aquaporins (AQP0-AQP12), all found in humans, were divided into three subfamilies based on their functional properties, permeability profile and sequence homology (**Figure *1.1***) [8,9]:

(1) Classical or orthodox aquaporins (AQP0, 1, 2, 4, 5, 6 and 8) were thought initially to be water selective, however now is known that some also transport gases, hydrogen peroxide (AQP1, 5 and 8), ammonia (AQP8) and charged particles [3,8].
(2) Aquaglyceroporins (AQP3, 7, 9, 10) in addition to water are also permeable to glycerol, hydrogen peroxide and urea (AQP3), ammonia (AQP3, 7 and 9) and other neutral small solutes [3,8].
(3) Unorthodox aquaporins (AQP11 and AQP12) also called "S-aquaporins", "superaquaporins", "subcellular aquaporins" or "sip-like aquaporins" are located intracellularly. While AQP11 can permeate water, glycerol and hydrogen peroxide, the permeability of AQP12 permeability is still uncertain. AQP11 and AQP12 are distantly related paralogs having 20% homology with other human AQPs [3,4,8].

The last two aquaporins (AQP13 and AQP14) are not inserted in these subfamilies because they are only found in older mammal lineages [8] and are still poorly characterized.

Some AQPs (AQP1, AQP3, AQP5, AQP8, AQP9 and AQP11) comprised in the subfamilies described above also mediate the transport of hydrogen peroxide (H_2O_2) across cell membranes and were named peroxiporins [7,9].

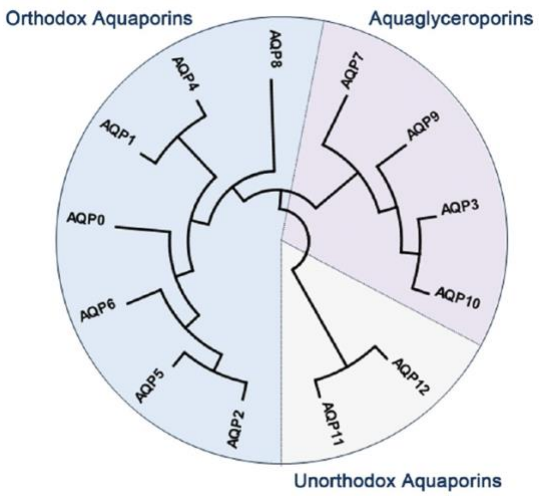

Figure 1.1: Dendrogram illustrating the phylogenetic relationship of mammalian cell AQPs, showing the three main subfamilies. (Adapted from [4]).

1.2.1 Aquaporin structure

AQPs from different categories of organisms were used to perform structural studies. The first AQP1 structure ever studied was determined by X-ray crystallography at 2.2 Å resolution, in 2001. This AQP1 was from red blood cells (RBCs) [10]. The results revealed a conserved aquaporin fold with six

transmembrane α-helices (M1, M2, M4, M5, M6 and M8), two half helices (M3 and M7), with their positive N-terminal ends located at the centre of the protein and their C-terminal ends facing the intracellular side of the membrane, and five connecting loops (loops a-e) surrounding a narrow water-conducting amphipathic channel in which water molecules align forming a single column [2,11,12]. Both N- and carboxyterminal groups are located intracellularly (**Figure *1.2*A**). [5]. In the membrane, four aquaporin molecules form a homotetramer (**Figure *1.2*B**), with each monomer ranging 26-34 kDa and forming a functional pore with 25 Å [1,8,11]. The arrangement of the four monomers creates an hydrophobic central pore that may facilitate gas transport (CO_2, NO) or can act as a cation channel [12].This tetrameric structure is common to all the AQP family, however at least one isoform, AQP4, can be combined in cell membranes into higher-order supramolecular assemblies known as orthogonal arrays of particles where the AQP4 tetramers are in square arrays and stabilized by interactions between the terminal amino acid residues of the monomers [11,13].

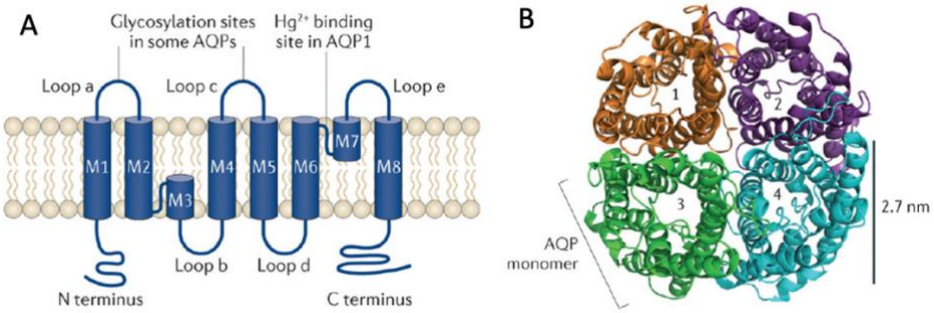

Figure 1.2: Structure of AQPs **A-** Topology map of the basic monomeric structure of an AQP showing the six transmembrane α-helices (M1, M2, M4, M5, M6 and M8) and the two half helices (M3 and M7) connected by the five loops (a-e). **B-** Top view of an aquaporin homotetramer with 4 identical monomers labelled 1-4. (Adapted from [11])

Each AQP monomer has a dumbbell-like shape structure and consists of an extracellular and cytoplasmatic vestibule connect by the amphipathic pore (**Figure *1.3*A**). Along the pore, there are two conserved constriction sites:

(1) aromatic/arginine selectivity filter (ar/R SF): this region is part of the extracellular vestibule being located near the periplasmic/extracellular entrance (**Figure *1.3*B**) and by being the narrowest region of the pore determines the size of the molecules allowed to pass through it. In orthodox subfamily of AQPs the ar/R SF is extremely narrow and is composed by four amino acids, usually Arg197, Phe 56, His182 and a fourth residue. In aquaglyceroporins the ar/R SF is only constituted by three amino acid residues, normally arginine, phenylalanine, and tryptophan, making the pore wider and allowing the passage of larger solutes. The ar/R constriction provides distinguishing features that allow the identification of AQPs from

different subfamilies by relating the size accessible for the passage of solutes with the residues that constitute this region. [2,10-12].

(2) Asparagine-proline-alanine (NPA) sequence motifs: the second constriction site is composed by 2 NPA sequence motifs located at the N-terminal ends of the two half-helices formed by loops B and E, and that contain inward-facing asparagine polar side chains. These motifs prevent the proton conduction, necessary to avoid dissipation of proton gradients, by being part of the hydrophilic surface of the amphipathic pore. There are some variants of this motif, for example, NPC in case of AQP11 and NPT in AQP12, both located intracellularly [2,11,12].

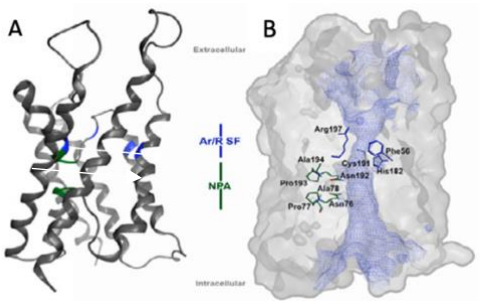

Figure 1.3: Structure of human AQP1s pore. **A-** Dumbbell-like shape structure of an AQP monomer displayed in ribbon. **B-** Channel surface represented as a blue mesh and ar/R SF and NPA regions indicated. (Adapted from [2])

1.2.2 Biological functions of AQP in mammals

AQPs are widely expressed all over the body, not only in tissues related to the transport of fluids but also in tissues that are not crucial for fluid movements. These proteins are involved in various biological functions, comprising brain edema, transepithelial fluid transport, proliferation, cell migration, metabolism, adhesion, and differentiation [4,11].

AQPs are known to act as important players in the physiology of several tissues and organs and consequently their altered expression is related with pathologies [14]. This information triggered the discovery of potential AQP modulators to be used for clinical applications. This work is focused on the physiological functions and modulation of the peroxiporin AQP3, aiming to investigate its role in melanoma skin cancer.

1.2.2.1 The skin structure and AQPs distribution

Skin is known to be the largest and most vulnerable organ in the human body by being the first line of defense that covers the entire external body surface. This organ plays several essential roles in immunological surveillance, thermoregulation, sensation and in some biochemical processes such as the production of Vitamin D_3 in consequence to the exposure to ultraviolet irradiation. Human skin has

a complex structure comprising three major layers (epidermis, dermis, and hypodermis), each one with resident cells with different characteristics (**Figure *1.4***):

(1) Epidermis: outermost layer of the skin and is composed essentially of keratinocytes originated in the Stratum Basale (SB) before differentiating and moving to the surface of the epidermis, but first passing through the Stratum Spinosum (SS) and Stratum Granulosum (SG). Once they reach the surface, these cells shed into the environment as dead skin cells in Stratum Corneum (SC). This layer is also colonized by other cells, like pressure-sensing Merkel cells, pigment-containing melanocytes, and antigen-processing Langerhans cells.

(2) Dermis: this layer is connected to the lower end of epidermis. Contains fewer cells and is mainly composed of the fibrous protein's collagen and elastin.

(3) Hypodermis: deepest layer of skin. Consists predominantly of adipocytes supported by a collagen-based structure named interlobular septa [14,15].

Pilosebaceous follicles, sweat glands, nerves and lymphatic blood vessels also take part of the structure of the skin [14].

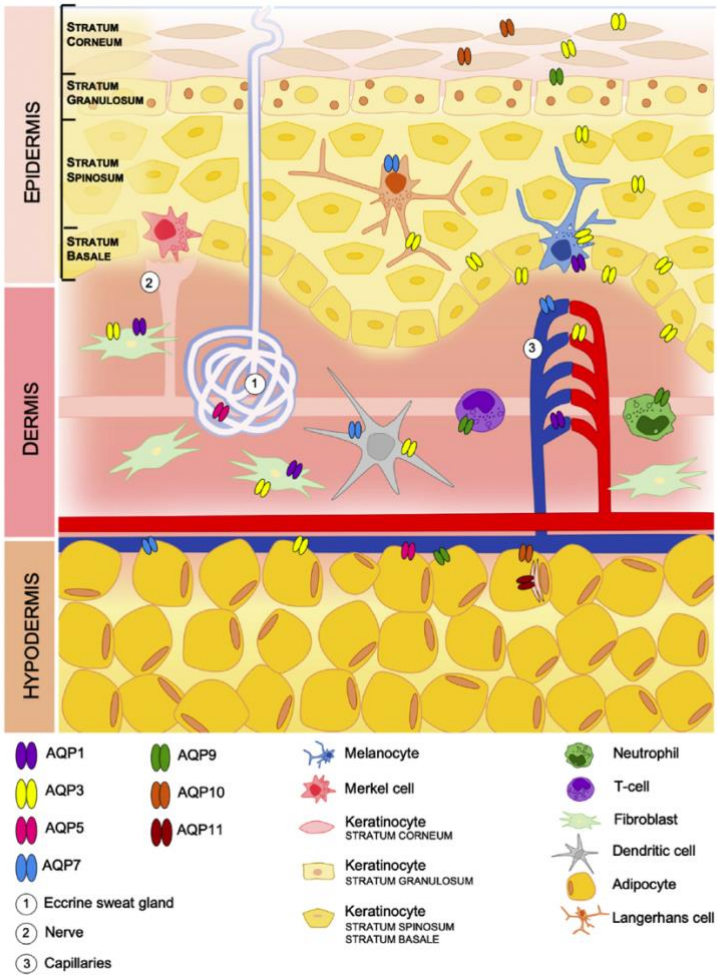

Figure 1.4: Schematic representation of the skin structure containing its three major layers, each one comprising particular cell types with distinct features and the AQP distribution according to each skin-resident cell type. (Adapted from [14])

Various AQPs are being detected in resident-skin cells at both at protein and transcript form. Deregulation of this AQPs is known to be linked with multiple skin pathologies, such as melanoma. AQP1, AQP3, AQP5, AQP7, AQP9 and AQP10 are expressed in the three principal skin layers, however only the AQPs located in the epidermis and glands, AQP3 and AQP5, are known to be more relevant for skin physiology [14].

1.2.2.2 AQP3 in the skin

AQP3 is constitutively active as water transporter on the basolateral, blood-facing, cell membranes [11]. This channel is expressed in multiple healthy human epithelia and cancer tissues (**Figure *1.5***) [16]. In the skin, AQP3 has a major role in skin hydration, wound healing, lipid metabolism and regulation of the proliferation and differentiation of keratinocytes. These last properties are related to its ability to transport glycerol [17].

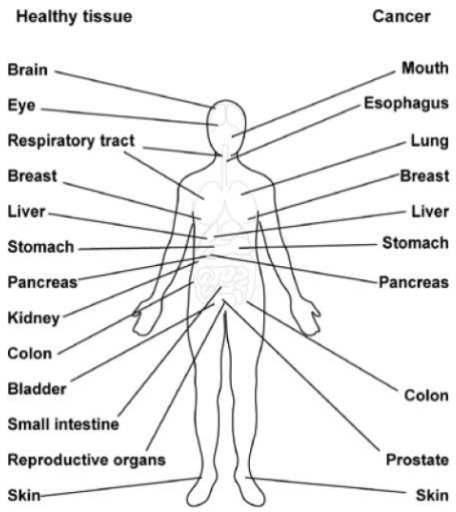

Figure 1.5: Schematic showing examples of AQP3 expression sites as well as examples of cancers, where increased expression of these water channel has been reported. (Adapted from [16])

Studies in AQP3-KO mice showed that AQP3-deficient mice have poor SC hydration that is not improved by exposing the skin to high humidity environments but by administering glycerol by topical or systemic routes. It was also discovered that the glycerol content of these mice is reduced when compared to the control mice. These observations led to the conclusion that AQP3 acts as a facilitator of glycerol permeation by controlling this molecule content in epidermis. Glycerol transported by AQP3 plays a key role in skin hydration. It diffuses from the deepest layer of epidermis to its surface, acting as a humectant dragging water along with it. This process increases the skin capacity to hold water guaranteeing the optimal hydration of all epidermis layers (**Figure *1.6*A**). In addition, in cultured

keratinocytes and human epidermis AQP3 also promotes urea uptake. Urea is known as an endogenous metabolite that enhances SC hydration [14].

AQP3 is also associated with wound healing and epidermal barrier repair. The SC is responsible for the barrier function. Due to its natural exfoliation and uninterrupted keratinocyte differentiation and proliferation; the SC layer of epidermis is in constant renovation. In the other hand, the wound healing ability of the skin is associated to the conservation of the barrier function. Hara-Chikuma and Verkman showed a decreased keratinocyte migration and wound healing in AQP3-KO mice. However, it was possible to reestablish keratinocyte migration after transfecting the cells with either AQP1 or AQP3 gene. This investigation revealed that AQP3 is crucial for cell proliferation and migration, contributing to skin wound closure [14].

In AQP3-defective epidermis was observed a reduction of the cell proliferation due to the reduction of the metabolism of those cells [14]. Glycerol can be converted in glycerol-3-phosphate by a glycerol kinase, that in turn will lead to the formation of ATP [14,18]. Hara-Chikuma and Verkman showed that AQP3 deficiency led to reductions of epidermal cell glycerol, its metabolite glycerol-3-phosphate and ATP without impairment mitochondrial function [19]. These findings confirm that glycerol permeation via AQP3 is crucial for cell proliferation in epidermis regeneration after injury since it provides the energy necessary to allow the wound closure (**Figure *1.6*B**) [14]. The impaired wound healing detected in AQP3-KO mice epidermis shows a association between AQP3 and tumor formation in mice confirming the mechanism referred before. [14,18]. Beside glycerol-3-phosphate, glycerol is also involved in lipid metabolism. Without AQP3 is also associated with the production of phosphatidylglycerol (PG) by providing glycerol to phospholipase D2 (PLD_2). PG is an activator of protein kinase C which in turn regulates AQP3 trafficking [14].

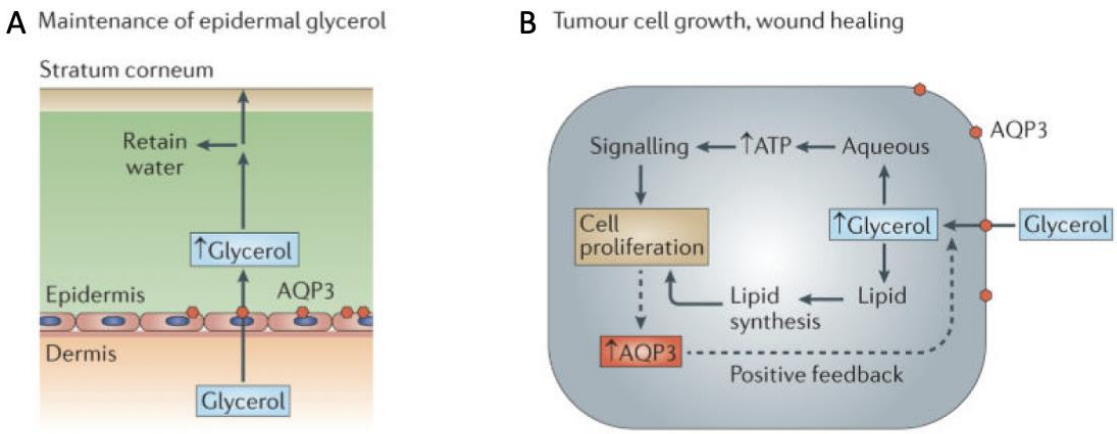

Figure 1.6: Physiological functions of AQP3. **A-** AQP3 facilitates skin hydration by maintaining high glycerol levels acting as a humectant to retain water in the SC. **B-** AQP3 maintains high glycerol cellular levels to produce ATP and lipid biosynthesis, leading to cell proliferation. (Adapted from [11])

In conclusion, AQP3 as a water and glycerol channel has a crucial role in fluid homeostasis and in cell metabolism. Additionally, AQP3 is also involved in the regulation of cell migration, differentiation and proliferation. As a consequence, is crucial for skin homeostasis and repair [14].

1.2.3 Aquaporins in cancer

Cancer is one of the leading causes of death worldwide and the incidence of this disease is increasing gradually across the years. Up-to-date treatments comprise surgery, chemotherapy and radiation therapy all of them associated to multiple side effects including loss of bone density, nausea, decreased fertility and premature menopause, painful neuropathy and increased risk of cardiovascular disease. The main focus of cancer treatments consists of inhibiting proliferation, while the major cause of death is cancer metastasis. The process of metastasis occurs when cells migrate from the primary tumor to distant organs. In the metastatic cascade there are some phases vulnerable to intervention such as detachment of cells from the primary tumor and infiltration of dissociated tumor cells into and out of circulatory pathways, first via intravasation and then via extravasation, and angiogenesis. By combining strategies that inhibit cancer proliferation and control metastasis of tumor cells, it may be possible to achieve less devastating cancer therapies [8]. Recently, the role of AQPs in cancer development has been studied. Studies revealed that tumor growth, development, invasion and metastasis rely on tumor metabolism and microenvironment. It is also well-known that AQPs have an important role in tissue water balance in response to osmotic gradients which is important to maintain cell function both in healthy and malignant cells [4].

Metastasis only occurs when a series of linked sequential steps are completed by tumor cells (**Figure *1.7***). Angiogenesis stimulates cancer invasion and metastasis. It is activated in response to hypoxia environments, where the oxygen perfusion is inadequate, triggering extracellular matrix breakdown, endothelial cell proliferation, migration, differentiation and recruitment of periendothelial cells. These cells, by forming discontinuous layers around vessels, exert developmental and homeostatic control. Angiogenesis can happen under physiological conditions, including skeletal muscle following physical activity, and in pathological scenarios such as tumorigenesis. In tumorigenesis, tissue hypoxia leads to the formation of new blood vessels, granting tumors to obtain nutrients, exchange gases and excrete metabolic waste (**Error! Reference source not found.**). Studies revealed that tumors with maximum 2 mm in diameter can survive via passive diffusion from surrounding tissue, however angiogenesis was crucial to support tumors with larger dimensions. It is also known that AQP1 is

involved in angiogenesis. This water channel, in response to the lack of oxygen , known to be upregulated by angiogenic factors enhancing endothelial cell migration and angiogenesis [8].

Like angiogenesis, epithelial-mesenchymal transition (EMT) also takes place in normal physiological conditions, for example implantation, embryogenesis and organ development, in addition to pathological processes such as cancer invasion and metastasis (**Figure *1.7***). In EMT the polarized epithelial cells pass through some biochemical changes in order to adopt a mesenchymal morphology. This phenotype is characterized by loss of cell polarity due to the alteration from apical-basal polarity to a more front-rear polarity, reduced cell-cell adhesiveness and enhanced invasive capacity [8,16]. The epidermal growth factor (EGF), hepatocyte-derived growth factor (HGF), platelet-derived growth factor (PDGF) and transforming growth factor beta (TGF-β) are some of the signals from the tumour-associated stroma that can induce EMT in cancer by stimulating transcription factors that act as epithelial cadherin (E-cadherin) transcription repressors. E-cadherin is a transmembrane glycoprotein crucial for the calcium-depended tight adhesions between epithelial cells and cytoskeleton elements. Downregulation of the protein is a hallmark feature of EMT. Some classes of AQPs have been associated with the EMT process, for example, AQP3 up-regulation in response to EGF in colorectal, gastric and pancreatic cancers is related with increased cell migration, invasion and metastasis [8].

An important aspect of cancer metastasis is the capacity to destroy the extracellular matrix (ECM) invading the neighboring tissue (**Figure *1.7***) [16]. Cell invasion implicates the translocation of cells through fluids or tissues enabling migration which is essential for tissue repair, physiological morphogenesis and immunity. In physiological conditions, the migration peak occurs during development and morphogenesis of mammalian cells and drops after terminal differentiation. However, in cancer cells migration machinery can be reactivated by chemokines released from host tissues and growth factors such as EGF secreted by stromal cells. Cancer cell migration and invasion can be induced by the expression of AQPs such as AQPs-1, 3, 4, 5, 8 and 9 [8]. Studies suggested that AQP redistribution to the leading edge of migrating cells lead to cell swelling, by promoting water and ions uptake, that facilitates forward movement because of the generation of increased space for actin filaments [4,16]. Peroxiporins have been linked with cancer cell migration, but to this point H_2O_2 transport has only been associated to AQP3 as a control mechanism in tumor cell migration [8,16]. In addition, AQPs may also stimulate cell-matrix adhesion, important to tumor cell spread and migration [4].

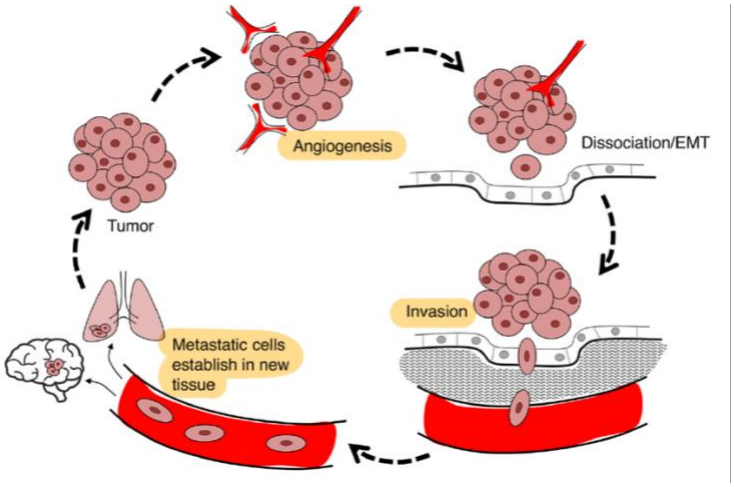

Figure 1.7: Diagram summarizing the steps in cancer metastasis. (Adapted from [8])

It is known that AQPs facilitate the uptake of permeants such as glycerol and hydrogen peroxide. These permeants may interact with oncogenes/oncoproteins leading to the activation of intracellular signaling cascades that stimulate the transcription of genes involved in cell growth, transformation and survival, and consequently promotes tumor progression. Additionally, AQP expression in malignant cells can be advantageous for high metabolic turn-over or tumor-specific metabolic pathways needed for their survival [4].

In light of the above, AQPs can be closely related to cancer so the understanding of their possible role in the etiology of the disease is crucial for developing therapies where they can be used as potential therapeutic targets or for using AQPs as clinical markers for cancer prognostic and diagnostic [17].

1.2.3.1 Peroxiporins in cancer

The transport of H_2O_2 across cell membranes by peroxiporins has been considered the last milestone in the timeline of H_2O_2 in biochemistry [7]. Hydrogen peroxide is a small molecule produced by aerobic metabolism or in response to extracellular insults and belongs to the reactive oxygen species (ROS) family [7,9]. H_2O_2 passage through AQPs can be explained by its chemical and physico-chemical properties that are comparable to those of water [19]. According to its concentration and localization this molecule can act as signaling molecule or as an oxidative stressor (**Figure *1.8***) [7,8]. Under physiological conditions (1-10 nM) H_2O_2 is the only ROS capable of moving out of the mitochondria playing an important role as a second messenger diffusing through cells and tissues in order to initiate immediate cellular effects, such as initiation of proliferation cell shape changes and recruitment of immune cells [19,20]. This role is denoted as oxidative eustress. At higher concentrations induce adaptative stress responses via master switches like Nrf2/Keap1 or NF-κB [20]. Supraphysiological

concentrations of H_2O_2 (> 100 nM) lead to oxidative distress where the interaction of this reactive oxygen species with various cellular targets can cause cell damage or even cell death [7,20]. As previously stated, only some AQPs (AQP1, AQP3, AQP5, AQP8, AQP9 and AQP11) have peroxiporin activity, however their permeability varies increasing from aquaglyceroporins to orthodox aquaporins [7]. In conclusion, facilitated diffusion of H_2O_2 across biological membranes is suggested to play an essential part in the fine-tuning of cell oxidative status and its biological consequences [9].

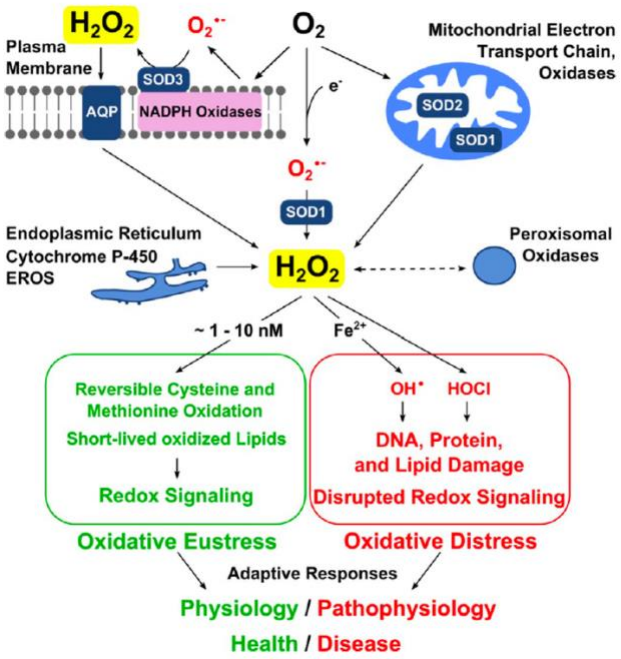

Figure 1.8: Role of hydrogen peroxide in oxidative stress and redox signalling. (Adapted from [20])

Redox signalling influences the pathophysiology of cancer. Cancer cells frequently present increased levels of ROS that can activate pro-tumorigenic signaling, enhancing cell survival and leading to DNA damage and genetic instability. In addition, in fast expanding tumors ROS are also generated from augmented oxidative metabolism and hypoxia [7]. Studies reported the overexpression of AQPs in human tumors from different origins. All the information presented before lead to the conclusion that peroxiporins represent new and promising targets for cancer therapies, since the channel-mediated membrane transport allows the fine adjustment of H_2O_2 levels [7].

1.2.3.2 AQP3 as potential therapeutic target in melanoma

Melanoma by having a high potential for metastasis is one of the most invasive and metastatic human cancers. As a consequence, it has the highest mortality rate of all dermatological cancers [14]. This cancer arises from the malignant transformation of melanocytes, specialized pigmented cells found

essentially in epidermis in the border with dermis. Melanocytes have an important role in protecting us against UV light and confer pigmentation to the skin by producing melanin. In melanoma, these cells show decontrolled proliferative features [14,21]. Various factors contribute for the onset of this disease, namely sun exposure, genetic predisposition and immunosuppressive states. Between all human cancers, this skin cancer has the highest mutation burden, consequently, this biological heterogeneity permits cancer cells to resist and evade the adopted therapies. Therefore, despite the considerable advances on cancer clinical management, therapies against metastatic melanoma are not successful or is very common to observe relapses [21].

Recent studies reported AQPs as new players in the development of this skin cancer, being potential drug targets against melanoma. Primary and metastatic human melanomas were used to perform a screening of AQP gene expression and the results showed that 8 of the 13 AQP isoforms are expressed in melanoma cells, however increasing evidence strongly suggests that AQP3 plays a pivotal role in this cancer' progression and metastasis [14,16]. In fact, in an experiment involving AQP3-knockout mice, it was revealed that AQP3 is necessary for skin tumor development, since these mice shown to be resistant to tumor formation even after being exposed to a tumor initiator. A possible mechanism for the reduced skin tumorigenesis referred before is the AQP3-mediated H_2O_2 transport in the mice that do not express this peroxiporin, as results show that AQP3 is required for EGF-induced cell signaling and cancer development by a mechanism involving EGF-induced generation of extracellular H_2O_2 and its transport by AQP3 to the interior of the cells (**Figure *1.9***) [7,21]. The interaction between AQP3 and epidermal growth factor receptor (EGFR) lead to the formation of a signaling module that triggers Nox activation. Consequently, Nox generates a second messenger, H_2O_2, which in turn is transported into cells by AQP3. Inside melanoma cells, H_2O_2 oxidizes protein tyrosine phosphatases (PTPs) that in turn activate other pathways in order to reduce the natural degradation of HIF-1α/ HIF-2α increasing the expression of vascular endothelial growth factor (VEGF), an important regulator in tumor angiogenesis and vessel maturation, so promoting the tumor survival [7,22]. AQP3 also promotes cell proliferation by increasing the intracellular glycerol content, which enters glycolysis and contributes to ATP formation mitochondria, providing the energy necessary to the tumor cells. Furthermore, these peroxiporins may directly or indirectly activate AKT to increase MMPs, resulting in tumor invasion [22]. These findings suggest AQP3 as a potential new therapeutic target in melanoma therapy [7].

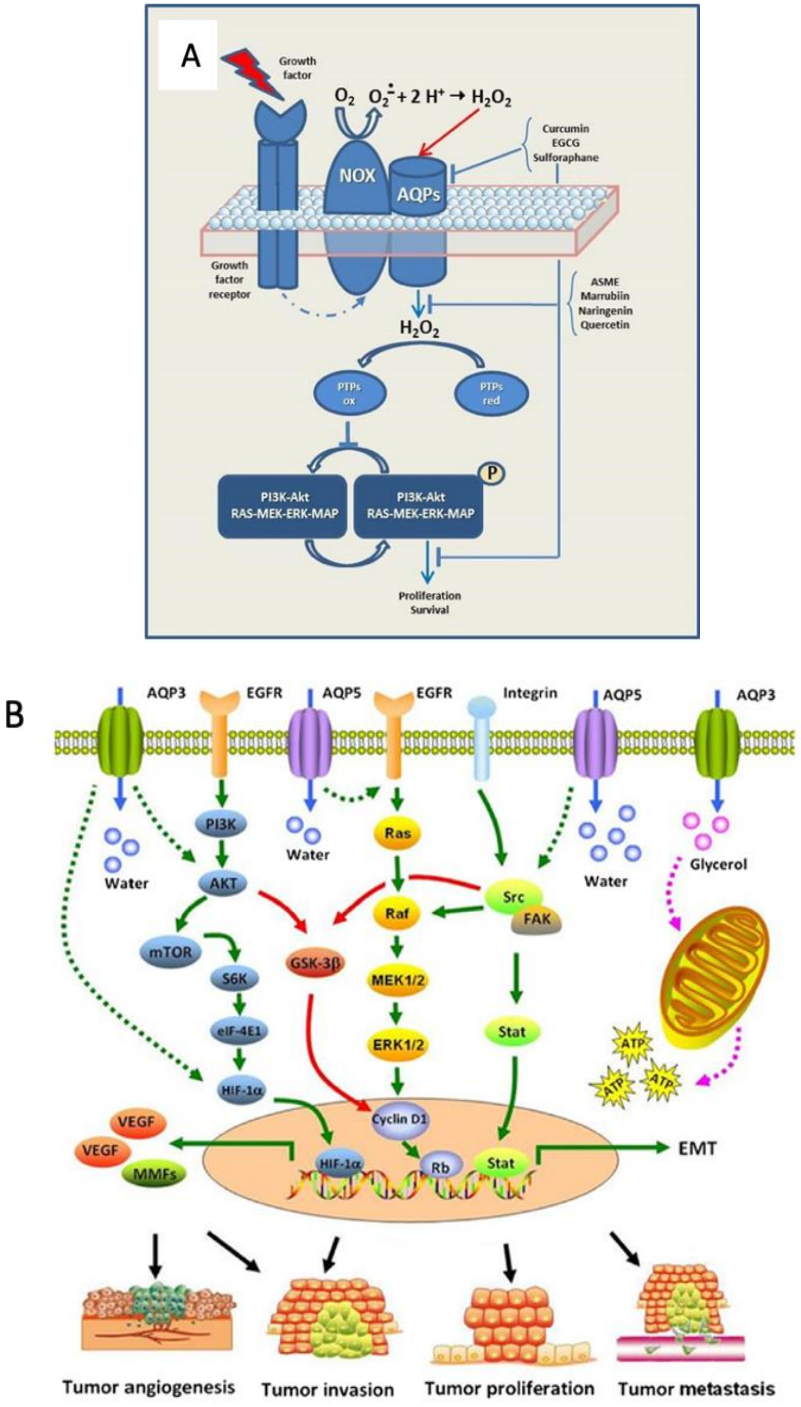

Figure 1.9: Model of novel roles of AQP3 in tumour biology. **A-**AQP3 as a potential new therapeutic target in melanoma therapy involving EGF/EGFR cell signalling. (Adapted from [7]). **B-** AQP3 role in tumour angiogenesis, invasion and proliferation. (Adapted from [22])

These results showed that AQP3 is an important biomarker for the diagnostic of skin cancers, such as melanoma [22].

1.3 Aquaporin modulators

To maintain homeostasis, cells may have to regulate the water permeability of their membranes [23]. A key property of aquaporin-mediated transport is its capability to be regulated in response to environmental or cellular signals, such as membrane tension, pH or hormones. Members of the AQP family are regulated at the individual protein level by two different mechanisms: through a conformational change, also called gating, or by changing the aquaporin density in a specific membrane [12,23]. The latter implicates regulation at the transcriptional/translational level in addition to trafficking where the protein molecules are recycled between the plasma membrane and vesicle pools [12,24]. The aquaporins from mammals are much more frequently regulated by the dynamic control of their subcellular localization then they are by gating because the first option has a faster time of response [24]. Considering their participation in normal and diseased physiological states, the modulation of aquaporin regulation has shown therapeutic potential in several health conditions, including cancer, revealing AQPs as potential drug targets [2,21]. Despite being promising therapeutic targets, the identification of AQP modulators for therapeutic and diagnosis purposes has proved to be a demanding task. Up to date, four classes of AQP-targeted agents have been described: (1) heavy metal-based inhibitors, (2) small molecules that are considered as water conductance inhibitors, (3) small molecules that target the interaction between AQP4 and the neuromyelitis optica (NMO) autoantibody and (4) agents acting as chemical chaperones, causing AQP2 mutants [11, 21]. The lack of selectivity and low efficiency of most of the modulators lead to an urgent need to find higher potency and selectivity aquaporin inhibitors with minimum toxicity to reduce the severe side effects caused by those molecules. Since this work is focused on the role of AQP3 in melanoma, the present chapter will be focused on the AQP3 inhibitors identified so far, more specifically on the gold-based compounds.

1.3.1 Gold-based compounds as AQP3 inhibitors

The coordination metal complexes are compounds that contain a central metal ion bound to organic ligands. Currently, the list of therapeutically prescribed metal-containing complexes comprises several metal compounds containing: silver (antimicrobial), bismuth (antiulcer), vanadium (antidiabetic), platinum (anticancer), antimony (antiprotozoal), iron (anticancer and antimalarial) and gold (antiarthritic) [1].

In 2013, Soveral and Casini reported several gold (III) complexes with N-donor ligands with high potency and selectivity for inhibiting aquaglyceroporin isoforms, namely AQP3 [2]. These compounds were tested for their inhibition properties of human AQP1 and AQP3. The results revealed that the Au (III) compounds were able to potently inhibit glycerol transport in human red blood cells not having a

significant effect on water transport [1]. Other studies revealed that the compounds do not have any effect on the permeability of AQP1 in different cell models, proving that these gold-based compounds are selective for aquaglyceroporins [2]. The lead compound of the series, Auphen ([Au(phen)Cl_2]Cl, phen= 1,10-phenantronile), is the most potent inhibitor of the group of Au-compounds with an IC_{50} in the low micromolar range (0.8 ± 0.008 μM). To gain insight into the mechanism of AQP3 inhibition by gold compounds, it was build a homology model of human AQP3 that was then compared to the structure of human AQP1. This comparison allowed the identification and characterization of protein binding pockets. Since gold has high affinity to sulphur, the mechanism of inhibition of Auphen and analogues is based in the interaction between Au (III) and the sulphur donor groups of AQPs, for example the thiolate of cysteine or the thioether of methionine residues. AQP3 has one thiol group of Cys40 located above the ar/R restriction site inside the protein pore projected toward the extracellular space [1,25]. Therefore, it seems that by binding to the residue previously described Auphen and the other gold compounds from the series can block the passage of glycerol via AQP3. The pore activity of this AQP after incubation with Auphen can be regained by using 2-mercapoethanol that act as a reducing agent [25,26].

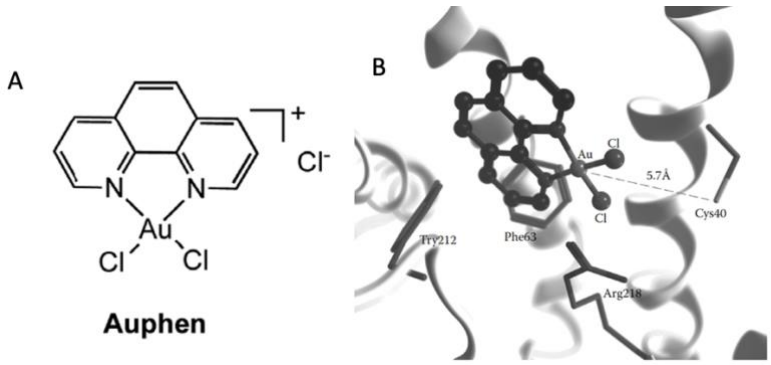

Figure 1.10: Auphen as inhibitor of aquaglyceroporins. **A-** Auphen chemical structure. (Adapted from [25]) **B-** Position of Auphen in the ar/R selectivity filter of AQP3 in direction of Cys40. (Adapted from [1])

The Auphen capacity of inhibiting cell proliferation not only in healthy but also in some cancer cell lines with different levels of AQP3 expression was examined. The results revealed that Auphen antiproliferative activity was directly associated with AQP3 expression by specifically disturbing AQP3-mediated glycerol permeability [21,26]. Overall, this information suggests that AQP3-targeted therapy with gold compounds may be helpful and effective in AQP3-overexpressing cancers, such as melanoma [1].

More recently, AQP3 was reported to also permeate H_2O_2 in addition to water and glycerol, being included in the peroxiporin sub-group [8]. This feature may explain its abnormal expression level in tumor cells and contribution to tumorigenesis.

2 Thesis Aims

The main goal of this project is to study AQP3 aquaglyceroporin and peroxiporin activities in melanoma cells and its contribution to cancer biology. In addition, this thesis aims to validate AQP3 as a drug target for anti-cancer therapeutics.

First, the most expressed AQP isoforms in MNT-1 and A375 melanoma cell lines will be identified by performing a Western Blot and a RT-qPCR assay. The results will assure that AQP3 is the target and will allow to choose the adequate inhibitors to perform the following assays.

The cytotoxicity of the selected gold-based compounds will be accessed by a colorimetric MTT assay. After identifying the proper concentration of inhibitor to be used on the assays, the inhibitory effect of these compounds on the permeability to water, glycerol and H_2O_2 in melanoma cells will be accessed by epifluorescence microscopy.

Subsequently, the effect of the gold-based inhibitors on melanoma cells adhesion and proliferation will be again evaluated by a MTT colorimetric assay, while the effect on cell migration will be accessed by a wound closure assay.

Lastly, to understand if the compounds under study induce cell death via apoptosis, it will be performed a LDH assay.

3 Materials and Methods

3.1 MNT-1 cell culture

In this project, two cell lines with distinct malignancies and of highly pigmented melanoma cells (MNT-1 and A375) were used. These cells were cultured in minimal essential medium, Dulbecco's Modified Eagle Medium (DMEM) (Lonza Biowhittaker®), supplemented with 10% (v/v) fetal bovine serum (FBS) (Gibco® Invitrogen) and 1% (v/v) penicillin-streptomycin (P/S) (Lonza Biowhittaker®), that was previously prepared and heated before defrosting the cells. After collecting the cell criovials from the nitrogen container (VWR), where they were stored, the cells were placed to thaw in a bath heated to 37°C, and 8 mL of DMEM was added to the defrosted cells. Then, the cells in suspension were centrifuged (Heraeus Sepatech Labofuge Ae) at 1000 rpm for 5 minutes. After centrifugation, the pellet was resuspended in 6 mL of DMEM (previously CO_2-equilibrated at 37°C in a humidified atmosphere of 5% CO_2, Sanyo CO_2 Incubator). At the end, the MNT-1 and A375 cells were maintained in a T-flask in the incubator, with the conditions, described above.

For trypsinization, first, the medium was discarded and cells were washed twice with 3 mL of phosphate buffered saline (PBS). Next, 0,5 mL of trypsin/EDTA 0,5% (v/v) (170 000U/L – Lonza Biowhittaker®) were added to the T-flask that was posteriorly placed in the incubator for 5 minutes. After the incubation time, 6 mL of DMEM, supplemented like described before, were added to resuspend the cells. The resuspension medium was then transferred to a 15 mL falcon and the cells were centrifuged at 1000 rpm for 5 minutes. During centrifugation step, 50 μL of the cell suspension were mixed with 50 μL trypan blue solution (Sigma-Aldrich®). Then, 50 μL of this solution were inserted in a hemocytometer (Neubauer chamber BLAUBRAND®) to perform a cell count using an inverted microscope (GX Microscopes). When the centrifugation was finished, the MNT-1 and A375 pellets were resuspended in 6 mL of DMEM and the inoculums of 10 000 cells/cm^2 and 15 000 cells/cm^2, respectively, were added to the corresponding T-flask. The cells were maintained in the incubator at 37°C in a humidified atmosphere of 5% CO_2 in air. Cells were used for experiments at a confluency of 80-90%.

In case there were to many cells for the intended assays, the remaining cells were frozen to maintain the cell bank. For that, 1mL of freezing medium was prepared consisting of 700 μL of DMEM, 200 μL of FBS and 100 μL of DMSO (AppliChem) and 1 million cells were added to this medium. Then, the vials were inserted in a Mr. Frosty™, that was at room temperature and filled with isopropanol, and stored at -80°C. In the next day, cells were moved to the nitrogen container for long storage.

All cell culture practices were performed under sterile conditions, in a laminar flow chamber (Sanyo Clean Bench) with an UV light, that was turned on for 20 minutes before every usage, for sterilization. All disposable materials used, as well as the DMEM medium, the FBS and the P/S antibiotic were supplied under sterile conditions.

3.2 RNA extraction and RT-qPCR

The reverse-transcription quantitative PCR (RT-qPCR) technique was used to analyze the expression of AQPs in both MNT-1 and A375 cell lines. This method allows the quantification of DNA, at each amplification cycle, in real time [27].

For the RNA extraction, cells were washed with 2 mL of PBS and centrifuged for 5 minutes at 1000 rpm. After the addition of 500 μL of TRIzol (Invitrogen), the cells were stored at -80°C. On the extraction day, 100 μL of chloroform were added to the defrost solution that was then centrifuged at 10 000 rpm for 15 minutes at 4°C. After collecting the RNA-containing aqueous phase, the RNA was precipitated by the addition of 250 μL of isopropanol that was left to rest for 10 minutes at room temperature and then, centrifuged at 10 000 rpm for 10 minutes at 4°C. Once removed the supernatant, 500 μL of ethanol at 75% were added centrifuged at 1000 rpm for 5 minutes at 4°C to wash the RNA. The last step was performed twice. Afterwards, the supernatant was discarded and the RNA was left to dry for 30 minutes. When dried, the RNA was resuspended in diethylpyrocarbonate (DEPC) water and placed in a dry bath at 55°C for 10 minutes.

The reverse transcription reaction was performed with 1000ng of RNA. To quantify the RNA extracted from the cells, 1 μL of each sample was analyzed in a Nanodrop equipment (NanoDrop®) using the program ND1000 V3.3.0. Knowing the concentration of RNA, calculations were made to have a mix with a final volume of 20 μL: 8 μL of sample, 10 μL of reaction mix (NZYTech Kit) and 2 μL of enzyme mix (NZYTech Kit). RT was performed in the thermocycler (Biorad) using the following PCR program:

(1) 25°C, 10 minutes
(2) 50°C, 30 minutes
(3) 85°C, 5 minutes
(4) 4°C, ∞

After the end of the first program, the remaining RNA was degraded by adding 1 μL of RNAse H (NZYTech Kit) and the second program was initiated:

(1) 37°C, 20 minutes

(2) 4°C, ∞

For the RT-qPCR assay, 15 mixes were prepared, one for the gene of each AQP (AQP0 – AQP12), β-actin and HPRT-1 gene. For each sample, mix was composed by 10 μL 2x TaqMan MasterMix (Applied Biosytems) and 1 μL 20x Taqman Assay. When all the mixes were prepared, a 96-well plate was prepared by adding 11 μL of mix and 9 μL of cDNA for each cell line, MNT-1 and A375. After performing a spin down of the plate, the qPCR program, was started:

(1) 50°C, 2 min
(2) 95°C, 10 min
(3) (95°C, 15 seconds followed by 60 °C, 1 minute) x 40 cycles
(4) 4°C, ∞

3.3 Western blot

3.3.1 Sample preparation for extraction

First, the samples stored at -80°C and the RIPA were defrosted. Then, to each sample were added 50 μL of RIPA and 1% of proteases inhibitor (0,5 μL). Next, the samples were resuspended 10 times, with a syringe and needle, and centrifuged at 12000 rpm for 30 minutes at 4°C. The resulting supernatant and pellet were stored in separate, at -80°C.

3.3.2 Protein quantification

Several concentrations of bovine serum albumin (BSA) were prepared (0; 0.5; 1; 1.5; 2 mg/mL) to obtain a calibration curve. The revealing agent was prepared by adding 8 mL of solution A to 160 μL of solution B from the kit in a ration Solution A: Solution B of 50:1. Next, 1 mL of the revealing solution was added to each standard/sample, and then incubated for 30 minutes at 37°C. After the incubation, the absorbances were measured at 562 nm. Once the total protein was quantified, calculations were made to know the volumes needed to have 5, 50 and 80 μg of protein for each cell line to use in western blot.

3.3.3 Gel preparation

First, the gels were prepared according to **Table *3.1***. Polymerizing agents (PSA and TEMED) are the last components to be added to the mixture right before place it in the molds. Once the separating gel was polymerized, the PSA and TEMED were added to the stacking gel, that then was placed in the

mold. Lastly, the comb was carefully inserted in the structure before the polymerization of the stacking gel.

Table 3.1: Volumes of the components used to prepare the separation and concentration gels.

	Separating gel (10%)	Stacking gel (5%)
Total volume (mL)	10	4
H_2O	3.96	2.24
30% Acrylamide	3.33	0.67
1.5 M Tris (pH 8.8)	2.50	1.01
SDS 10%	0.10	0.04
PSA 10%	0.10	0.04
TEMED	0.010	0.004

3.3.4 Sample preparation

For the sample preparation, were added 6 μL of loading buffer (ration sample:LB – 4:1) to the already diluted protein sample. Subsequently, the samples were denatured in a dry bath at 95°C for 5 minutes. At the end, a spin down of the samples was performed and they were left on ice.

3.3.5 Protein electrophoresis

Once the stacking gel was polymerized, the support containing the gels was placed in the electrophoresis tank. After adding the running buffer to the electrophoresis tank, the comb was removed and 20 μL of each sample were added. A molecular marker Precision Plus Protein Dual Color Standards (BioRad) ran in parallel with the samples. The electrophoresis ran at 80 V until the samples reach the separating gel and then it ran at 120 V for the rest of the time.

3.3.6 Sample transfer

First, the membrane was inserted in methanol for 1 minute, to be activated, and then washed in H_2O. Then, it was placed in transfer buffer for 10 minutes. Once the electrophoresis was finished, the gel was also placed in transfer buffer for 10 minutes. Then, the transfer stack was mounted, and proteins were allowed to transfer for 2 hours at 250 A.

3.3.7 Blocking and antibody labelling

After transfer, the membrane was blocked in TBS-T with 5% skimmed milk, for 1 hour with agitation. During the incubation time, the dilutions of the primary antibodies for AQP3 (1:200) and α-tubulin (1:1000) were prepared in TBS-T with 3% BSA. Finally, the membranes were inserted in falcons with the respective primary antibodies and were left in agitation at 4°C overnight. In the next day, the membranes were washed with TBS-T 3 times for 5 minutes. Next, the membranes were incubated with the secondary antibody diluted in blocking solution for 1 hour with agitation. The anti-mouse secondary antibody was used in a dilution of 1:10000. Lastly, the membranes were washed 3 times for 5 minutes with TBS-T.

To reveal the membrane, a revealing solution composed by 400 μL hydrogen peroxide and 400 μL luminol was prepared. Bands were captured using a Chemidoc in chemiluminescence mode,

3.4 MTT assay

The MTT (3-(4,5-dimethylthiazol-2-yl)-2,5-diphenyltetrazolium bromide) tetrazolium assay is used to measure metabolic activity as an indicator of cell viability. The same compound was also used to investigate the effect of AQP3 blockage on cytotoxicity, cell adhesion and proliferation. This test is based on the enzymatic reduction of the yellow-colored tetrazolium salt to its formazan form of intense purple color (**Figure *3.1***), which can be quantified spectrophotometrically [28]. In human cells, MTT is reduced in the mitochondria of viable cells with active metabolism by mitochondrial enzymes [29].

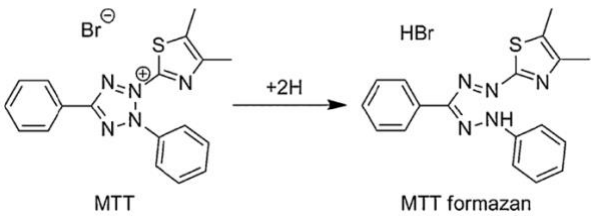

Figure 3.1: Reduction of MTT bromide to its formazan. (Adapted from [28])

For this assay, a MTT solution of 0,5 mg/mL was prepared with MTT (Sigma-Aldrich®) and PBS. After removing the medium from the cells, they were washed with 100 μL of PBS and then 100 μL of the MTT previously prepared were added to wells. When the plates were finished, they were placed in the incubator at 37°C in a humidified atmosphere of 5% CO_2. Once the incubation time was over, the MTT was removed and 50 μL of DMSO were added to the cells that then incubated under agitation for 10 minutes. At the end of the incubation time the microplate was inserted in a microplate reader (BMG LABTECH) and the absorbance was recorded at 570 and 690 nm.

3.4.1 Cytotoxicity assay

Cytotoxicity, as well as adhesion, proliferation and migration, were studied under the same conditions. In these assays, 3 inhibitors from the family of Auphen were used in parallel with three different controls (**Figure *3.2***). The chosen compounds were the $[Au(C^{CO}N)Cl_2]$ ($C^{CO}N$ = 2-benzoylpyridine), $[Au(C^{NH}N)Cl_2]$ ($C^{NH}N$ = N phenylpyridine-2-amine) and $[Au(C^{CH2}N)Cl_2]$ ($C^{CH2}N$ = 2-benzylpyridine) (**Figure *3.2***), here referred as $C^{CO}N$, $C^{NH}N$ and $C^{CH2}N$ respectively. These compounds were synthetised in Angela Casini's laboratory, in the Technical University of Munich.

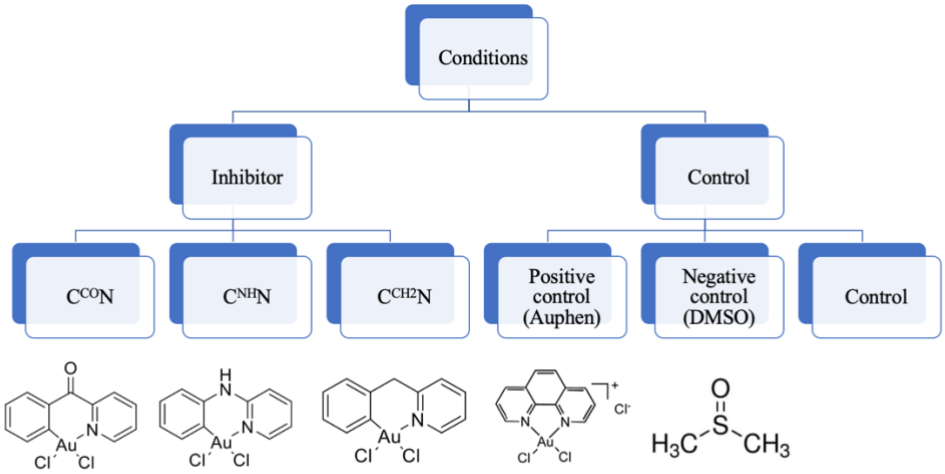

Figure 3.2: Schematic representation of the conditions used in the cytotoxicity, adhesion, proliferation and migration assays. The chemical structures of the compounds used are represented under the respective compound.

For the cytotoxicity assay, the initial step was the preparation of two 96-well plates with an inoculum of 40 000 cells/cm^2 for both MNT-1 and A375 cells. After 24 hours, the cells were incubated with a series of dilutions of the compounds under study: 0, 2.5, 5, 7.5 and 10 μM. After 24 hours of incubation, a MTT assay was performed as described above. The incubation time with MTT was 1 hour.

3.5 Permeability assays

3.5.1 Permeability to water and glycerol

The permeability of melanoma cells to water and glycerol was assessed using calcein-acetoxymethylester (calcein-AM). This compound Calcein-AM has no fluorescence and is cell permeant. Once inside viable cells, intracellular esterases convert the permeable molecule into calcein, a cell impermeant anionic and volume sensitive fluorophore (**Figure *3.3***) [30]. Calcein was used to

study water and glycerol permeability in MNT-1 and A375 cells, since it allows to follow cell volume changes during time.

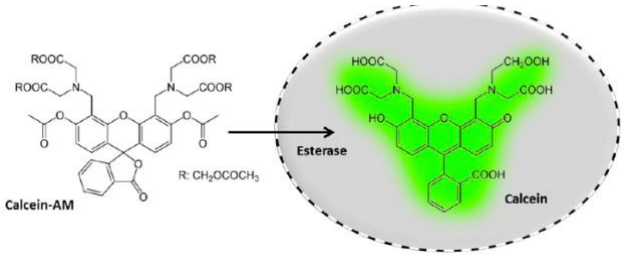

Figure 3.3: Scheme of the change from calcein-AM to its fluorescent form. (Adapted from [31])

For the experiment, a inoculum of 20 000 cells/cm^2 was inoculated in fluorescence-specific coverslips for the MNT-1 cell line, and for the A375 cell line was inoculated an inoculum of 160 000 cells/cm^2. In the following day, cells were washed with PBS 1x prior to incubation with 2 mM of Calcein-AM (Sigma-Aldrich®) in routine DMEM, for 30 minutes, at 37°C, 5% CO_2. When evaluating the inhibitors ($C^{CO}N$, $C^{NH}N$, $C^{CH2}N$, Auphen), cell treatment was performed in parallel with the last 10 minutes of Calcein-AM incubation. The excess of probe was washed with the 300 mOsm buffer HEPES.

The cover slips with the adherent MNT-1 and A375 cells were mounted in a perfusion chamber (Warner Instruments, Hamden, USA) and sealed with a new cover slip and an O-ring. The perfusion chamber was then mounted on an inverted epifluorescence microscope (Axiovert 200 Zeiss), equipped with a CCD digital camera (Cool Snap^{TM} EZ Photometrics). A 40x oil immersion objective was used. The cells were excited at 495/10 nm, with a Xenon lamp, with an interval between pulses of 1s at a frequency of 1Hz. Fluorescence emission was detected at 515/10 nm through a dichroic filter. All the signals obtained were stored on an external computer and analyzed using Metafluor software (Molecular devices, USA).

The buffer solutions were previously placed in the reservoirs of a syringe system. Initially, cells were equilibrated in buffer HEPES 300 mOsm. Then, this solution was replaced by HEPES buffer with mannitol 300 mOsm, a hypertonic solution with an impermeant solute. After reaching the new osmotic equilibrium, the solution was replaced by HEPES buffer so that the cells regain their initial volume. Finally, HEPES was replaced by HEPES buffer with glycerol 300 mOsm, a hypertonic solution with a permeant solute, to achieve an external osmolarity of 600 mOsM.

All steps related to Calcein handling were carried out in the absence of light or using a red light.

3.5.2 Cell measurements

Cell measurements were performed to convert fluorescence signals to relative volumes. For that, an inoculum of 15 000 cells/cm^2 was allowed to grow for 24h in 6-well plates, and in the next day, the

cells of one well were trypsinized and centrifuged at 1000 rpm for 5 minutes. Then, the pellet was resuspended in 1mL of PBS and centrifuged at 100 rpm for 5 minutes. Then, the cells were resuspended with 20μL of the buffer 300 mOsm HEPES and a drop of the suspension was added to a glassslide. Cell pictures were acquired in the microscope (Axiovert 200 Zeiss) with the 40x oil-immersion objective. The experiment was repeated in cells resuspended in 300 mOsm HEPES buffer with 300 mM Mannitol to define the cell minimal volume for a challenge of tonicity 2. The width of the cells was measured using the ImageJ software. Two perpendicular diameter measurements were registered for each cell.

3.5.2.1 Conversion of fluorescence signal to relative volume and estimation of permeability parameters

The fluorescence signals collected reflect the changes in cell volume when cells are confronted with an hyperosmotic solution and the decay of the fluorescence emission. Each fluorescence signal corresponding to a single cell was treated individually. In order to estimate water (P_f) and glycerol (P_{gly}) permeability coefficients, fluorescence raw data was converted in fluorescence signals by subtracting the background signal. Then, the fluorescence signals (F) obtained were rearranged to obtain the relative variation F/F_0. F_0 was obtained for each signal as an average of F values that correspond to the fluorescence emitted by cells in steady state, immediately before the osmotic challenge. Equation 1 shows the direct relationship between the variation of the relative cell volume (V/V_0) and the variation of the fluorescence signal (F/F_0), where (a) is the slope and (b) the ordinate.

$$\frac{V}{V_0} = a \times \frac{F}{F_0} + b \qquad \text{(Equation 3.1)}$$

The cell measurements performed were used to obtain cell volumes. In cells whose cell volume measurements were performed using HEPES, the volume was measured at the time corresponding to the introduction of the osmotic perturbation (V_0) and in those whose perturbation was performed using HEPES with mannitol, the volume was measured at the time corresponding to the end of the perturbation (V_{inf}).

Data of relative volume vs time obtained was then analyzed using a mathematical model implemented in the Berkeley Madonna software containing the equations:

$$J_v = P_f \left(\frac{V_w A}{RT}\right)(-\Delta\Pi_S - \Delta\Pi_{ND}) \quad (\text{cm}^3\ \text{s}^{-1}) \qquad \text{(Equation 3.2)}$$

$$J_S = P_{gly}\Delta C_S A \quad (\text{mol}\ \text{s}^{-1}) \qquad \text{(Equation 3.3)}$$

Equation 2 and 3 are the simplified flux equations for water (J_v) and diffusible solutes (J_S) from the inner to the outer compartment. V_w corresponds to the partial molar volume of water (18 $cm^3\ mol^{-1}$), R

is the perfect gas constant, T is the temperature (298K) and A corresponds to the total membrane area (cm^2), $\Delta\Pi_{S,ND}$ are the osmotic pressure gradients due to concentration gradients of diffusible (S) and non-diffusible (ND) solutes [32].

Through mathematical models that simulate the dynamic behavior of cells when exposed to the osmotic shocks it was possible to estimate the permeability parameters through the settlement of theoretical curves with experimental curves of cell volume variation, using the experimental data.

3.5.3 Permeability to hydrogen peroxide

The generation of ROS can be detected by several biochemical approaches. 2',7'-dichlorodihydrofluorescein diacetate (H_2DCFDA) is a chemically reduced form of fluorescein that indicates the presence of ROS in cells. After the action of by intracellular esterases, that lead to the cleavage of the acetate groups, and oxidation, the non-fluorescent molecule is converted to 2',7'-dichlorofluorescein (DCF), a highly ROS-sensitive fluorescent compound [30]. This molecule was used to study the H_2O_2 permeability of MNT-1 and A375 cells.

First, a solution of 100 μM H_2O_2 was prepared as follows. To 1mL HEPES 300 mOsm was added 1 μL H_2O_2.Then, 500 μL of the previous solution was added to 1 mL HEPES 300 mOsm.

For this experiment cells were incubated with 2 mM H_2DCF in routine DMEM, for 30 minutes, 5% CO_2 Inhibitors were added in the last 10 minutes of the fluorophore incubation. After the incubation, cells were mounted in the perfusion chamber with 145 μL HEPES 300 mOsmand placed ate the stage of an inverted epifluorescence microscope (Axiovert 200 Zeiss), equipped with a CCD digital camera (Cool Snap™ EZ Photometrics). Once the fluorescence signal stabilized, 5 μL H_2O_2 solution (final concentration) was added to the cells. Data acquisition was performed using a 40x oil immersion objective. The cells were excited at 495/10 nm, with a Xenon lamp, with an interval between pulses of 10s at a frequency of 1Hz and fluorescence emission was detected at 515/10 nm through a dichroic filter. All the signals obtained acquired using Metafluor software.

The H_2O_2 influx (P_{H2O2}) was measured by following the time course of ROS accumulation upon the H_2O_2 challenge. The influx referred before was reported as a first order rate constant obtained from the slope of a semi-logarithmic plot of fluorescence intensity vs. time.

3.6 Adhesion assay

For the adhesion assay, an inoculum of 10 000 cells/cm^2 (MNT-1) or 15 000 cells/cm^2 (A375) was used. Cells resuspended in DMEM supplemented with 10% FBS and 1% P/S were then allowed to adhere in the following conditions:

- 2 mL of cell suspension
- 2 mL of cell suspension and 10 μM Auphen
- 2 mL of cell suspension and 5μM DMSO, $C^{CO}N$, $C^{NH}N$ or $C^{CH2}N$

For each condition, 6 replicates were made for each condition of each cell line, and cells were incubated at 37°C in a humidified atmosphere of 5% CO_2. In this experiment, 2 timepoints were verified, 3 and 6 hours after incubation. In each timepoint, the rate of adhesion was assessed by a MTT assay, as described above. The incubation time of MTT was 2 hours.

3.7 Proliferation assay

Contrary to the adhesion assay, where compounds are added to the media when cells are still in suspension (to evaluate their influence in cell adhesion), in the proliferation assays, compounds are added to the adherent cells, since the effect under evaluation is cell division.

For the proliferation assay, an inoculum of 10 000 cells/cm^2 or 15 000 cells/cm^2 was used for MNT1 and A375, respectively. Cells were resuspended in DMEM supplemented with 10% FBS and 1% P/S, inoculated and allowed to adhere for 24 hours. Then, adherent cells were treated according to the following conditions:

- 2 mL of DMEM supplemented with 10% FBS and 1% P/S
- 2 mL of DMEM supplemented with 10% FBS and 1% P/S and 10 μM Auphen
- 2 mL of DMEM supplemented with 10% FBS and 1% P/S and 5μM DMSO, $C^{CO}N$, $C^{NH}N$ or $C^{CH2}N$

Cells were incubated in a humidified atmosphere of 5% CO_2 at 37°C. After incubation, an MTT assay was performed according to the protocol previously described and with an incubation time with MTT of 2 hours. For each condition, 6 replicates were prepared and 3 timepoints (21, 27 and 45h) were evaluated.

3.8 Migration assay

MNT-1 and A375 cells were seeded in 12-well plates with an inoculum of 30 000 cells/cm^2 and 60 000 cells/cm^2, respectively. In the next day, a scratch was done in the cell monolayer using a sterile

10 µL tip. Then media was renewed to remove cell debris. Cells were treated with 5uM $C^{CO}N$, $C^{NH}N$ and $C^{CH2}N$, and 10uM Auphen (positive control). DMSO was used as the negative control (inhibitors solvent).

Three photos of each wound were taken using the inverted microscope (GX Microscopes) and the software GXCapture-T at 0, 9 and 24h after the scratch. The wound closure analyses were performed using the ImageJ software. For each image, three wound width measurements were collected.

3.9 LDH assay

The lactate dehydrogenase (LDH) assay was used to determine if the inhibitors $C^{CO}N$, $C^{NH}N$ and $C^{CH2}N$ have apoptotic properties. In cells undergoing apoptosis, necrosis and other forms of cellular damage that interfere with membrane integrity, LDH, a stable cytoplasmatic enzyme, is quickly released into the cell culture supernatant [33]. The LDH activity can be determined in an enzymatic test. First, lactate is converted to pyruvate by LDH leading to reduction of NAD^+ to $NADH/H^+$. In the second reaction, diaphorase (catalyst) transfers H/H^+ from $NADH/H^+$ to the tetrazolium salt INT, that in turn, is reduced to formazan. In brief, this protocol measures the reduction of a yellow tetrazolium salt into a red water-soluble formazan dye whose absorbance can be measured at 492 nm (**Figure *3.4***). By measuring the formazan formed it is possible to know the number of dead or damaged cells.

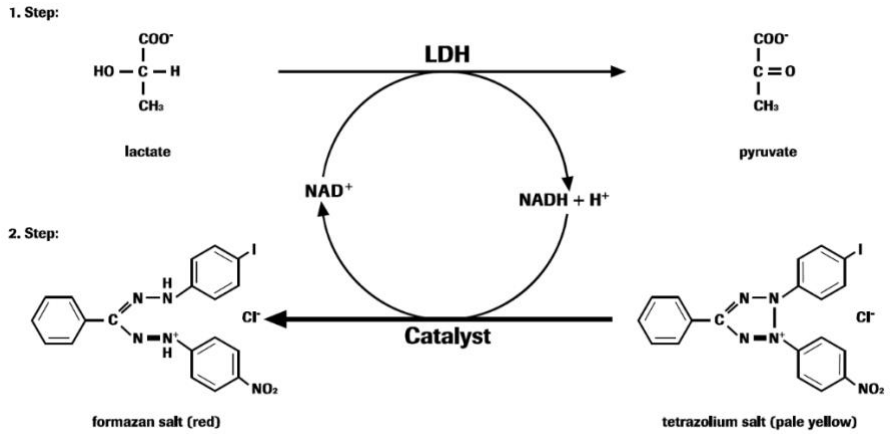

Figure 3.4: Reactions involved in the LDH assay. (Adapted from [34])

First, a 12-well plate was prepared with an inoculum of 30 000 cells/cm^2. Once the cells were confluent, the following solutions were prepared:

- 1.5 mL of Opti-MEM (Gibco® Invitrogen) and 5 μM $C^{CO}N$
- 1.5 mL of Opti-MEM and 5 μM $C^{NH}N$
- 1.5 mL of Opti-MEM and 5 μM $C^{CH2}N$

Then, 500 μL of Opti-MEM were added to the control wells, and in the inhibitor containing wells were added 500 μL of the corresponding solution from the solutions prepared previously. After 24 hours of incubation the supernatants of the control and inhibitor wells were collected, and the cells of the positive control were collected with 100 μL of radioimmunoprecipitation assay buffer (RIPA). Once the cells were collected, were performed 6 cycles of 5 seconds in the vortex. Then, all the samples were centrifuged for 10 minutes at 1000 rpm and the supernatant was collected. Next, the samples were prepared and added to a 96-well plate:

- 80 μL of ET buffer and 20 μL of the positive control (LDH collected from the inside of cells by promoting cells lysis with RIPA)
- 50 μL of ET buffer and 50 μL of the inhibitors and control (LDH collected from the supernatant of cells that were not treated with any of the inhibitors)
- 100 of ET tampon

The reaction mix was prepared by adding the reagent 1 and 2 from the Cytotoxicity Detection Kit^{PLUS} (LDH) (Roche) in a proportion of 1:45 and 100 μL of this mix were added to each well of the 96-well plate. After 30 minutes of incubation the absorbance was measured at 492 and 690 nm when the absorbance of the positive control at 492 nm reached a value of 2.5-3.

3.10 Statistical analysis

All experiments were performed in at least two biological and two technical replicates. Data are presented as means $\pm$ standard error of the mean (SEM). The statistical analysis performed between groups was made by two-way ANOVA and non-parametric Mann–Whitney test. A p-value <0.05 was considered statistically significant. All the statistical analyses were performed using the software Graph Prism (GraphPad Software).

4 Results and Discussion

4.1 AQPs expression in human melanoma cells

To define which AQPs were expressed by melanoma cells, the expression of AQP isoforms was screened in MNT-1 and A375 cells by quantitative PCR. As depicted in **Figure *4.1***, AQP11 and AQP3 are the most expressed isoforms in both melanoma cell lines. AQP1 and AQP5 are also expressed at lower levels in these cells. In A375 cell line, the isoforms AQP4, AQP6, AQP7 and AQP8 were also detected.

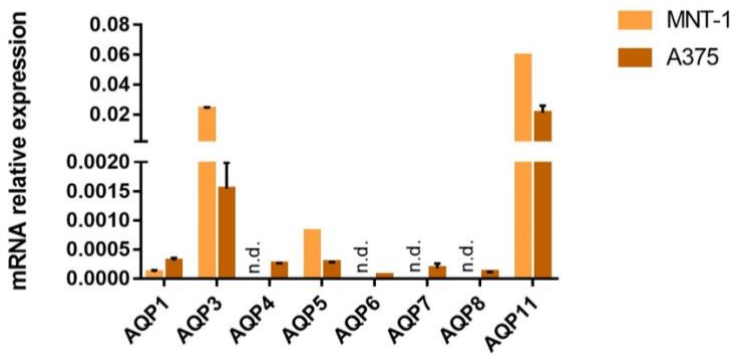

Figure 4.1: Screening of AQPs expression in MNT-1 and A375 human melanoma cells. AQP mRNA relative expression in melanoma cells was normalized to the mean of two housekeeping genes, HTRP-1 and β-actin. Data shows AQP3 and AQP11 as the most expressed isoforms in both cell lines. Data represent means $\pm$ SEM of one experiment. n.d., not detected.

A study by Gao et al. showed that over 50% of the melanoma cell lines they used in their study aberrantly expressed AQP11 and AQP3 [35]. The RT-qPCR results obtained here (**Figure *4.1***) are in accordance with the former study since the two melanoma cell lines under study, MNT-1 and A375, both primary melanoma cell lines, express high levels of AQP11 and AQP3. These results show that both isoforms can be used as biomarkers for melanoma detection and can be considered as potential drug targets for therapy. However, since AQP11 is mostly localized intracellularly [4], AQP3 has a greater potential as a drug target being more accessible to inhibitors.

4.2 AQP3 protein expression in human melanoma cells

After concluding that AQP3 is one of the most expressed AQP isoforms in both melanoma cell lines, a Western Blot was performed to confirm the high AQP3 expression at the protein level.

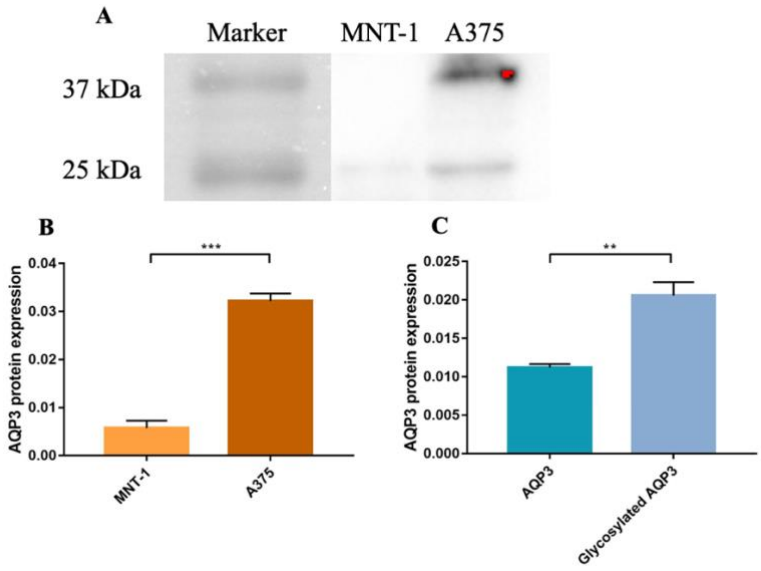

Figure 4.2: Protein expression of AQP3 in MNT-1 and A375 cells. **A-** Proteins have been isolated and a Western Blot was performed with antibodies direct against AQP3. The secondary antibodies used were anti-mouse. The molecular marker used was the Precision Plus Protein Dual Color Standards (BioRad). **B-** AQP3 protein expression in MNT-1 and A375 melanoma cells. **C-** AQP3 protein expression in A375 cells. Data represent means ± SEM of one experiment. **p< 0.01, *** p < 0.001.

As shown in **Figure *4.2***, the Western Blot results revealed a stripe at around 25 kDa. Since each AQP3 monomer have a molecular weight ranging 28 kDa, the stripe showed in **Figure *4.2*** is an indicator of the presence of AQP3 in both melanoma cell lines. The results also showed a stripe around 40 kDa in A375 cells that corresponds to AQP3 glycosylated form [36]. The effects of posttranslational modifications on AQP3 have not yet been investigated, however by analogy with AQP2, glycosylation may be required for membrane localization and can be an indicator of newly synthetised AQP3 [37,38].

The results showed that AQP3 mRNA expression in MNT-1 was higher than in A375 cells. However, according to **Figure *4.2***, in A375 cells, AQP3 protein is present in larger amounts than in MNT-1 cells. This reveals that probably in A375 cells the mRNA was already converted to protein, which explains its lower levels and massive amounts of AQP3 protein. In addition, MNT-1 are melanotic cells, while A375 are amenalotic cells, and a study showed that the absence of melanin is a sign of aggressiveness [39]. Therefore, A375 is considered a more aggressive cell line than MNT-1, which might explain the higher level of AQP3 protein expression, an oncogene candidate in melanoma. Once more, the results prove that AQP3 has a great potential as a drug target since it is highly both at mRNA and protein levels.

4.3 Cytotoxicity of organogold compounds in human melanoma cells

As the RT-qPCR and Western blot results revealed that AQP3 has the greatest potential for drug target and treatment of melanoma, we decided to investigate the effect of a family of organogold compounds on AQP3 activity and melanoma cells' biology. These compounds were cyclometalated Au (III) complexes with bidentate C^N ligands derived from Auphen, a known potent and selective inhibitor of AQP3 with antiproliferative activity [26,40]. The chosen compounds were the $C^{CO}N$, $C^{NH}N$ and $C^{CH2}N$.

In order to define the most suitable concentration of the compounds ($C^{CO}N$, $C^{NH}N$, $C^{CH2}N$ and Auphen) to be tested in all subsequent assays without comprising cell viability and avoid masking the results, their cytocixity was evaluated in MNT-1 and A375 cells. The compounds were tested at a range of concentrations and after 24 h of incubation the cell viability of MNT-1 and A375 cells was measured.

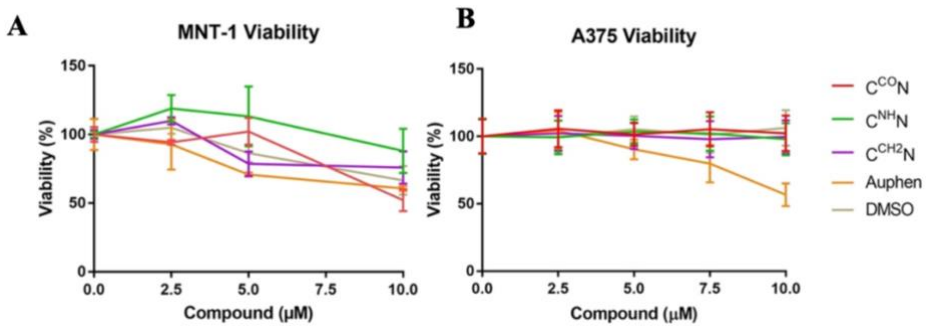

Figure 4.3: Effect of gold compounds on the viability of melanoma cells. Cell viability determined by MTT assay after cell exposure to the gold compounds for 24 h. **A –** MNT-1 cells viability incubated with gold compounds (0, 2.5, 5 and 10 μM for 24 h). These data were provided by Andreia G. Silva. **B –** A735 cells viability incubated with gold compounds (0, 2.5, 5, 7.5 and 10 μM for 24 h). Results are expressed as means ± SEM of three independent experiments.

As depicted in **Figure *4.3***, the maximum concentration at which the gold compounds are not toxic (maintaining at least 70% cell viability) to MNT-1 cells is 5 μM. Above this concentration, both $C^{CO}N$ and Auphen reduce cell viability, which indicates that they are toxic at higher concentrations. On the other hand, none of the gold compounds affected the viability of the A375 melanoma cells, even at a concentration of 10 μM, except Auphen which decreased cell viability above 5 μM. Based on these results, the concentration of inhibitors used in all the subsequent assays was 5 μM once it was the higher concentration for all the gold complexes did not impact on viability of both cell lines.

4.4 Effect of organogold compounds on the permeability of water and glycerol

To assess the potential inhibitory activity of Au (III) C^N complexes on AQP3 function, the effects of $C^{CO}N$, $C^{NH}N$ and $C^{CH2}N$ were studied on water and glycerol permeability in MNT-1 and A375 cells. To evaluate water permeability, cells were challenged with a hyperosmotic mannitol solution, which

created an osmotic gradient leading to a fast water efflux and, therefore, cell shrinkage since mannitol is a non-permeable solute. On the other hand, for glycerol permeability, was used a hyperosmotic glycerol solution to challenge the cells. As glycerol is a permeable solute in cells expressing aquaglyceroporins (e.g., AQP3), it induced a fast cell shrinkage due to osmotic water outflow followed by a reswelling caused by glycerol and water influx through AQP3 [41]. Pf and Pgly coefficients were both calculated using the mathematical models inserted in the Berkeley Madonna software.

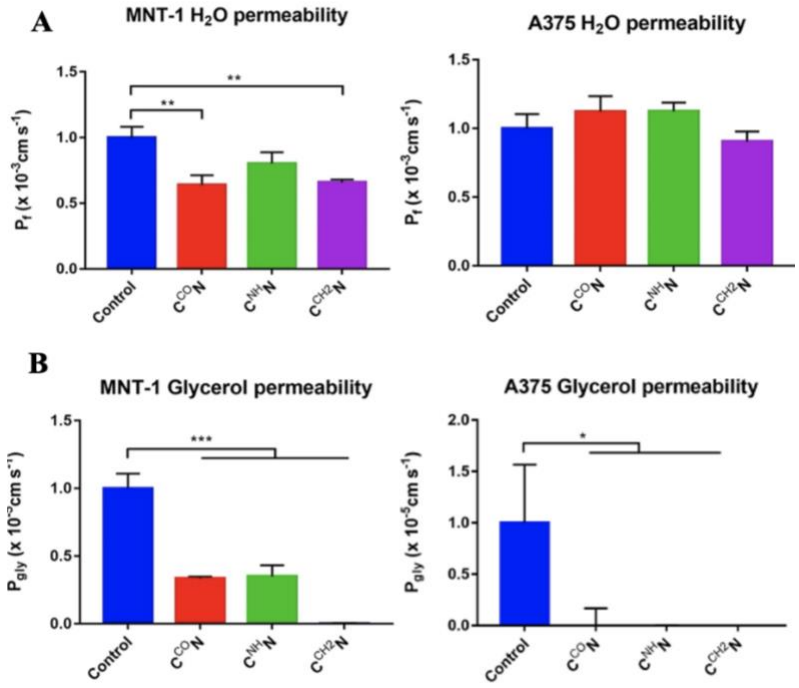

Figure 4.4: Effect of $C^{CO}N$, $C^{NH}N$ and $C^{CH2}N$ on melanoma cells permeability. Cell permeability determined by the incubation of melanoma cells with 10 μL of calcein-acetoxymethylester (calcein-AM) for 30 minutes. The data related to the compound $C^{CO}N$ in MNT-1 cells was provided by Andreia G. **A-** Water permeability of melanoma cells (MNT-1 and A375) incubated with gold compounds (5μM for 10 minutes). **B-** Glycerol permeability of melanoma cells (MNT-1 and A375) incubated with gold compounds (5μM for 10 minutes). Results are expressed as means $\pm$ SEM of two independent experiments. * $p < 0.05$, **$p< 0.01$, *** $p < 0.001$.

As illustrated in **Figure *4.4***, none of the compounds significantly affected A375 cell water permeability. However, $C^{CO}N$ and $C^{CH2}N$ affected water permeability in 36% and 34%, respectively, in MNT-1 cell line. These non-expected results might be explained by the lower AQP3 protein expression level of these cells. In fact, the increase of the molecular ratio [compound/AQP3] where the same amount of inhibitor molecules have lower number of AQP-protein to bind, may producing a global higher inhibition compared to A375 cells that express higher level of AQP3 protein. Glycerol permeability was affected by all the compounds under study in both cell lines, which indicates that these complexes reduce AQP3 glycerol channelling activity. $C^{CH2}N$ inhibited glycerol transport via AQP3 in MNT-1 cells in 100% and in the case of A375 cells $C^{CO}N$ was the best inhibitor by reducing AQP3 aquaglyceroporin activity to 0%. In a study by Pimpão et al., amongst the series of compounds $C^{CO}N$

resulted to be one of the most efficient to inhibit glycerol permeation in human AQP10 [40]. As seen in this work, in A375 cells this compound was also the one that most inhibited AQP3 activity.

Previous results showed that the impairment of glycerol transport via AQP3 caused by these gold complexes can potentially be used to deaccelerate the progression of melanoma. The uptake of glycerol by AQP3 in cancer cells provides a crucial molecule for metabolic reactions in energy demanding melanoma cells [22]. In addition, it is known that AQP3 plays a crucial role in skin hydration, wound closure and lipid metabolism, that are processes related to its ability of transporting glycerol [17]. By inhibiting the entry of this source of energy needed for cancer cells development, it is possible to impair their growth and spread, suggesting that the compounds under study may have a great antiproliferative activity and that AQP3 is a potential drug target for the treatment of melanoma.

4.5 Effect of organogold compounds on the permeability of hydrogen peroxide

As a peroxiporin, AQP3 can also transport hydrogen peroxide (H_2O_2). To fully understand the potential inhibitory activity of Au (III) C^N complexes on AQP3 function, the effects of $C^{CO}N$, $C^{NH}N$ and $C^{CH2}N$ on melanoma cells permeability to H_2O_2 was also evaluated. For that, cells were incubated with a fluorescent probe H_2DCFDA, which was used as an indicator of the presence of ROS inside the cells. The values of intracellular ROS accumulation rate after an external challenge with an isosmotic solution containing H_2O_2 were calculated from the slope of a semi-logarithmic plot of fluorescence intensity vs. time.

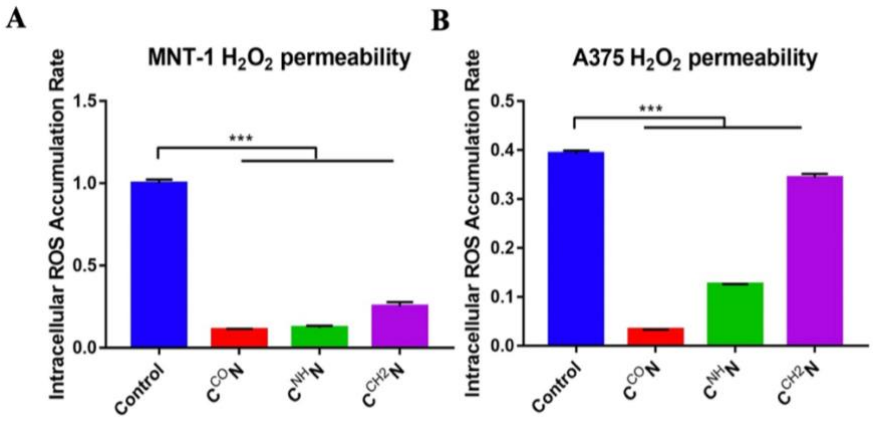

Figure 4.5: Effect of $C^{CO}N$, $C^{NH}N$ and $C^{CH2}N$ on melanoma cells permeability. Cell permeability determined by the incubation of melanoma cells with 10 μL of H_2DCFDA for 30 minutes. The data related to the compound $C^{CO}N$ in MNT-1 cells was provided by Andreia G. Silva. **A-** Hydrogen peroxide permeability of MNT-1 cells incubated with gold compounds (5μM for 10 minutes). **B-** Hydrogen peroxide permeability of A375 cells incubated with gold compounds (5μM for 10 minutes). Results are expressed as means ± SEM of two independent experiments. **p< 0.01 and *** p < 0.001.

As depicted in **Figure *4.5***, all the compounds significantly inhibited the accumulation rate of H_2O_2 in MNT-1 and A375 cells. For both MNT-1 and A375 cells, the best inhibitor of AQP3 peroxiporin activity was $C^{CO}N$ by inhibiting in 89 and 92%, respectively.

The data showed that organogold compounds disturbed the AQP3-mediated transport of H_2O_2. Once inside the cells, H_2O_2 can interact with oncogenes leading to an activation of pro-tumorigenic signalling, and therefore, enhance cancer cell survival. By inhibiting AQP3 peroxiporin activity and thus decreasing intracellular H_2O_2 content, PTPs would be less oxidised and in turn HIF-1α/ HIF-2α would be more degraded. Therefore, the decrease expression of VEGF would lead to an impairment of the angiogenesis promoting a decrease in melanoma cell proliferation or ever cell death [7,22].

4.6 Effect of organogold compounds on melanoma cell adhesion, proliferation and migration

To further investigate whether AQP3 inhibition by gold complexes underlie signal transduction mechanisms that affect melanoma progression, the melanoma cell adhesion, proliferation and migration were evaluated in the presence and absence of the inhibitors under study. Cell adhesion was evaluated by a MTT assay after cell exposure to 5 μM of organogold compounds, 3 and 6 hours after seeding the cells. MNT-1 and A375 cell adhesion was then normalized to the mean of the 3-hour result.

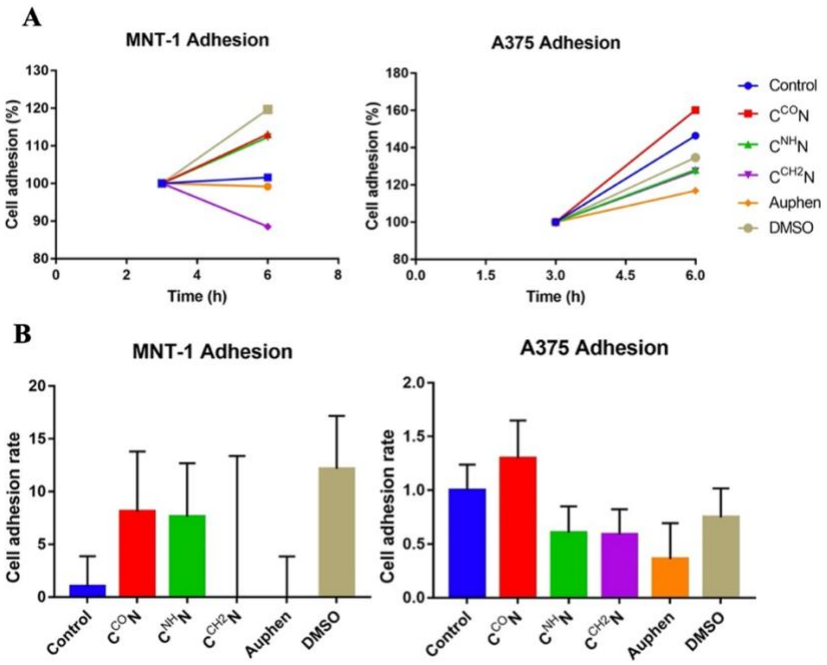

Figure 4.6: Effect of the AQP3 selective gold compounds on MNT-1 and A375 cell adhesion. Cell adhesion determined by 3-(4,5-dimethylthiazolyl-2)-2,5-diphenyltetrazium bromide (MTT) assay after cell exposure to 5 μM of AQP3 inhibitors 3 and 6 hours after cell adhesion Human melanoma cells adhesion normalized to the mean of the 3-hour result. Data represent means $\pm$ SEM of three (MNT-1) and two (A375) independent experiments.

As shown in **Figure *4.6***, none of the compounds significantly inhibited the adhesion of the melanoma cells. In both cell lines, $C^{CH2}N$ complex has showed a bigger tendency to inhibit cellular adhesion with a percentage of inhibition of 100% in MNT-1 cells and 41% in A375 cells. A study by Silva et al. showed that cells with silenced AQP3 and AQP5 had a lower cell-cell adhesion [42]. By inhibiting AQP3, the interactions between cells become weaker because the number of contacts stablished between them through adhesive molecules is lower. The results showed that the inhibition of AQP3 by the organogold compounds, can impair melanoma progression by weakening the connection between the cancer cells.

To evaluate melanoma cell proliferation, a MTT assay was performed after cell exposure to 5 μM of compounds at 3, 21, 27 and 45 hours after cell adhesion. MNT-1 and A375 proliferation was then normalized to the mean of the 3-hour result.

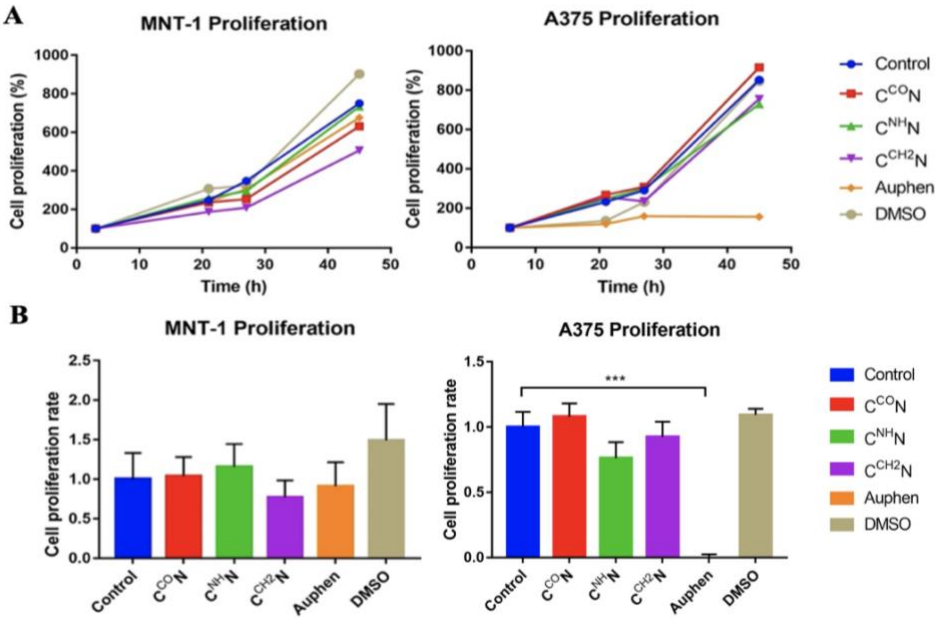

Figure 4.7: Effect of the AQP3 selective gold compounds on MNT-1 and A375 cell proliferation. Cell proliferation determined by MTT assay after cell exposure to 5 μM of AQP3 inhibitors at 3, 21, 27 and 45 hours after cell adhesion. Human melanoma cells adhesion normalized to the mean of the 3-hour result. Data represent means $\pm$ SEM of three (MNT-1) and two (A375) independent experiments. *** $p < 0.001$.

Again, none of the organogold complexes, except for Auphen in A375 cells have significantly inhibited cell proliferation (**Figure *4.7***). Auphen is known by its antiproliferative activity, so it was expected a higher inhibition of the proliferation by the gold complexes since they derive from Auphen. In MNT-1 cells the greater inhibition was of 23% in the presence of the $C^{CH2}N$ complex. Excluding Auphen, $C^{NH}N$ showed a higher inhibition of A375 cells proliferation with an inhibition of 24%.

In order to proliferate, cells require large amounts of energy. Once glycerol enters cells via AQP3 it goes through a lot of metabolic reactions leading to the formation of ATP in the mitochondria that in turn it will be used by tumour cells to perform several biological functions [22]. Additionally, by also facilitating the permeation of H_2O_2 and interacting with oncoproteins, AQP3 is postulated to activate intracellular signalling cascades that induce the transcription of important key genes involved in melanoma cell division and proliferation [42]. As said before, the impairment in glycerol and H_2O_2 transport via AQP3 by the gold complexes studied may lead to deacceleration of melanoma progression since MNT-1 and A375 proliferation would be decreased.

Cell migration was studied by performing a wound closure assay followed at 0, 9 and 24 h after opening of the wound. As depicted in **Figure *4.8***, all compounds have shown a tendency to delay melanoma cell migration compared to the control condition. In MNT-1 cells, $C^{CO}N$ led to an inhibition of the wound closure of 21%, being thus considered the best inhibitor. On the other hand, in A375 cells $C^{NH}N$ showed the higher inhibition level by inhibiting 22% of the wound closure.

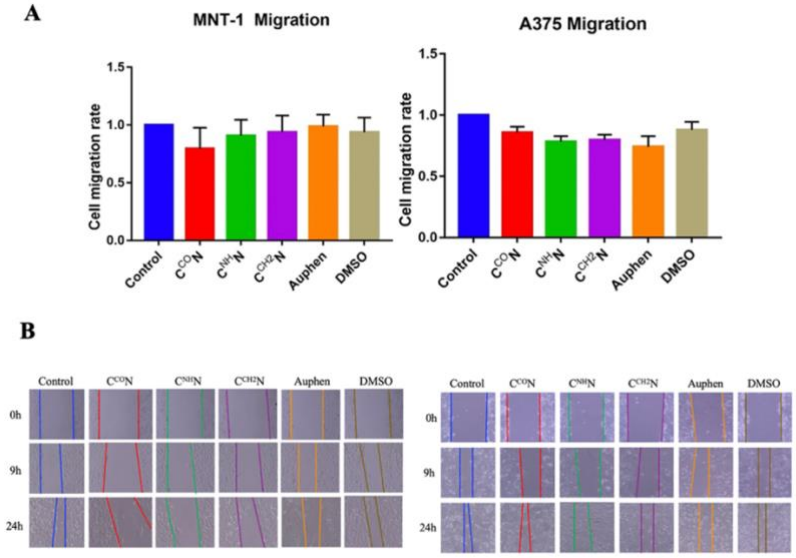

Figure 4.8: Effect of the AQP3 selective gold compounds on MNT-1 and A375 cell migration. **A-** Cell migration rate of cells non-treated (Control) and treated with 5 μM of AQP3 gold inhibitors. **B-** Representative images of wound closure progression in control and cells treated with 5 μM of AQP3 gold inhibitors. Results are expressed as means ±SEM of four (MNT-1) and three (A375) independent experiments.

Studies showed that cancer cell migration can be related to the higher expression of AQP3 [8]. The results from RT-qPCR showed that in the melanoma cell lines under study AQP3 is highly expressed, which is in agreement with the literature. In addition to the high level of AQP3, for the migration to occur, it is necessary a redistribution of these proteins to the leading edge of migrating cells to promote

water and ions uptake, inducing cell swelling. The increase in cell volume allows the generation of increased space for actin filaments, facilitating the forward movement [4,16]. The results illustrated in **Figure *4.8*** demonstrate that by inhibiting the AQP3 aquaglyceroporin and peroxiporin activities it is possible to reduce melanoma cell migration.

4.7 Effect of organogold compounds on melanoma cell membrane integrity

Membrane leakage is typically linked with cell death by necrosis or apoptosis [43]. A LDH colorimetric assay was performed to understand if the gold complexes studied compromise melanoma cells membrane integrity leading to apoptosis.

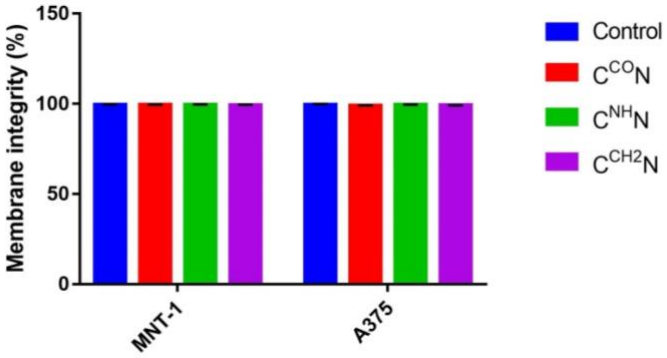

Figure 4.9: Effect of $C^{CO}N$, $C^{NH}N$ and $C^{CH2}N$ on membrane integrity of MNT-1 and A375 human melanoma cells. LDH release was quantified in the culture medium using the colorimetric method of the reduction of a yellow tetrazolium salt into a red water-soluble formazan dye. Data represent means ± SEM of two independent experiments.

As shown in **Figure *4.9***, none of the gold complexes damaged the melanoma cells membrane since the membrane integrity remained intact. The results show that the interaction of $C^{CO}N$, $C^{NH}N$ and $C^{CH2}N$ with AQP3 can interfere with MNT-1 and A375 cells ability to permeate glycerol and H_2O_2, and consequently, to adhere, proliferate and migrate without leading to cell death since no LDH leakage was detected.

According to the results obtained in this study, the gold compounds tested can inhibit the transport of glycerol and H_2O_2 via AQP3 without associated toxicity and promotion of melanoma cell death. In addition, by blocking AQP3 permeability these complexes have a tendency to impair cell adhesion, proliferation and migration. All these results suggest that the organogold compounds under study possess anticancer activities and are therefore potential candidates as anticancer drugs for melanoma treatment.

5 Conclusions

This thesis was focused on the assessment of AQP3 aquaglyceroporin and peroxiporin activities and their contribution to the biology of melanoma cells. In addition, it was also dedicated to the validation of AQP3 as a drug target for anti-cancer therapeutics by testing a series of gold inhibitors that could selectively target AQP3 and impair the cell processes responsible for cancer development such as cell adhesion, proliferation and migration.

In the first part of the thesis, the RT-qPCR and Western Blot results showed that AQP3 was amongst the most expressed AQP isoforms in both cell lines (MNT-1 and A375) and that AQP3 protein is present in larger quantities in A375 cells. This suggests that AQP3 can be used as a biomarker for the diagnostic of melanoma and that the inhibitors to be studied should be selective for AQP3.

On the second part of the thesis, the toxicity of the series of gold compounds selected ($C^{CO}N$, $C^{NH}N$ and $C^{CH2}N$) was evaluated to determine the ideal concentration of compound to be used in the cellular assays. The results showed that in A375 cells all the compounds, apart from Auphen, were not toxic in a concentration range up to 10 μM, while in MNT-1 cells, $C^{CO}N$ and Auphen showed toxicity at concentrations above 5 μM. Thus, all subsequent cellular assays were performed by treating cells with compounds at 5 μM.

In the third part of this work, the effect of the gold compounds on the membrane permeability to water, glycerol and H_2O_2 was studied in MNT-1 and A375 cells. Only $C^{CO}N$ and $C^{CH2}N$ affected MNT-1 ability of transporting water. In A375 cells none of the compounds impaired significantly AQP3 permeability to water. On the other hand, glycerol permeability was affected by all the compounds under study in both melanoma cell lines, which indicates that these complexes reduce AQP3 glycerol channelling activity. $C^{CH2}N$ and $C^{CO}N$ were the best inhibitors in MNT-1 and A375, respectively, and equally reduced AQP3 aquaglyceroporin activity to 0%. In both cell lines, the most potent inhibitor of H_2O_2 transport via AQP3 was $C^{CO}N$ by restraining AQP3 peroxiporin activity in 89% and 92%, respectively. These results show that the organogold compounds tested disturbed the AQP3-mediated transport of glycerol and hydrogen peroxide.

The inhibitory effect of gold compounds on human AQP3 was investigated in proliferation and migration. Melanoma cells migration was assessed by a wound closure assay. In both cell lines, $C^{CH2}N$ showed a larger tendency to reduce cell adhesion, 100% in MNT-1 and 41% in A375 cells. MNT-1 proliferation was compromised the most by $C^{CH2}N$ (23%) and $C^{CO}N$ induced a greater decrease on these cells' migration (21%). In A375 cell line, $C^{NH}N$ have shown a greater tendency of impairing cell proliferation and migration with an inhibition of 24% and 22%, respectively. These results revealed that the changes in cells' permeability to glycerol and to hydrogen peroxide affect the biology of melanoma cancer cells by affecting cell adhesion, migration and proliferation.

On the last part of the thesis, the effect of the organogold compounds on melanoma cell membrane integrity was assessed. The results obtained showed that none of the gold complexes studied disturbed

the membrane stability since there was no LDH released from cells. This proves that the interaction of $C^{CO}N$, $C^{NH}N$ and $C^{CH2}N$ with AQP3 interfere with cells permeability to glycerol and H_2O_2, impacting in proliferation and migration, without associated toxicity and cell death.

Table 5.1: Summary of the best candidate inhibitors and respective percentage of inhibition for each cell line and assay performed. MNT-1 (orange); A375 (brown); $C^{CO}N$ (red); $C^{NH}N$ (green); $C^{CH2}N$ (pink).

	MNT-1		A375	
	Inhibitor	Inhibition (%)	Inhibitor	Inhibition (%)
H_2O permeability	$C^{CO}N$	36%	$C^{CH2}N$	10%
Glycerol permeability	$C^{CH2}N$	100%	$C^{CO}N$	100%
H_2O_2 permeability	$C^{CO}N$	89%	$C^{CO}N$	92%
Cell adhesion	$C^{CH2}N$	100%	$C^{CH2}N$	41%
Cell proliferation	$C^{CH2}N$	23%	$C^{NH}N$	24%
Cell migration	$C^{CO}N$	21%	$C^{NH}N$	22%

Overall, the gold-based compounds herein tested revealed to be suitable drug candidates for melanoma, where AQP3 is highly expressed. In the future, it may be interesting to study the effect of $C^{CO}N$, $C^{NH}N$ and $C^{CH2}N$ on melanoma invasion and cell cycle to understand how these compounds affect cancer progression.

6 References

[1] G. Soveral, A. Casini, and S. Nielsen, *Aquaporins in health and disease : new molecular targets for drug discovery*. CRC Press, 2015

[2] G. Soveral and A. Casini, "Aquaporin modulators: a patent review (2010–2015)," *Expert Opinion on Therapeutic Patents*, vol. 27, no. 1, pp. 49–62, 2017. doi: 10.1080/13543776.2017.1236085.

[3] A. Madeira, T. F. Moura, and G. Soveral, "Detecting aquaporin function and regulation," *Frontiers in Chemistry*, vol. 4, 2016. doi: 10.3389/fchem.2016.00003.

[4] I. Direito, A. Madeira, M. A. Brito, and G. Soveral, "Aquaporin-5: From structure to function and dysfunction in cancer," *Cellular and Molecular Life Sciences*, 73: 1623–1640, 2016. doi: 10.1007/s00018-016-2142-0.

[5] R. N. Finn, J. Cerda`3, and C. Cerda`3, "Evolution and Functional Diversity of Aquaporins," *Biol. Bull.*, 229: 6-23, 2015.

[6] R. K. Singh, R. Deshmukh, M. Muthamilarasan, R. Rani, and M. Prasad, "Versatile roles of aquaporin in physiological processes and stress tolerance in plants," *Plant Physiology and Biochemistry*, vol. 149 : 178–189, 2020. doi: 10.1016/j.plaphy.2020.02.009.

[7] C. Prata, S. Hrelia, and D. Fiorentini, "Peroxiporins in cancer," *International Journal of Molecular Sciences*, vol. 20, no. 6, p. E1371, 2019. doi: 10.3390/ijms20061371.

[8] M. L. de Ieso and A. J. Yool, "Mechanisms of aquaporin-facilitated cancer invasion and metastasis," *Front Chem*, 6: 135, 2018, doi: 10.3389/fchem.2018.00135.

[9] C. Rodrigues *et al.*, "Human aquaporin-5 facilitates hydrogen peroxide permeation affecting adaption to oxidative stress and cancer cell migration," *Cancers (Basel)*, vol. 11, no. 7, pp. 1-17, 2019, doi: 10.3390/cancers11070932.

[10] H. Sui, B.-G. Han, J. K. Lee, P. Walian, and B. K. Jap, "Structural basis of water-specific transport through the AQP1 water channel," *Nature*, vol.414, no. 6866, pp.872-878, 2001.

[11] A. S. Verkman, M. O. Anderson, and M. C. Papadopoulos, "Aquaporins: Important but elusive drug targets," *Nature Reviews Drug Discovery*, vol. 13, no. 4., pp. 259–277, 2014. doi: 10.1038/nrd4226.

[12] S. Kreida and S. Törnroth-Horsefield, "Structural insights into aquaporin selectivity and regulation," *Current Opinion in Structural Biology*, vol. 33., pp. 126–134, 2015. doi: 10.1016/j.sbi.2015.08.004.

[13] A. Adeoye, A. Odugbemi, and T. Ajewole, "Structure and function of aquaporins: The membrane water channel proteins," *Biointerface Research in Applied Chemistry*, vol. 12, no. 1, pp. 690–705, 2022. doi: 10.33263/BRIAC121.690705.

[14] I. v. da Silva, A. G. Silva, C. Pimpão, and G. Soveral, "Skin aquaporins as druggable targets: Promoting health by addressing the disease," *Biochimie*, vol. 188, pp. 35–44, 2021. doi: 10.1016/j.biochi.2021.05.019.

[15] D. Sachs, A. Wahlsten, S. Kozerke, G. Restivo, and E. Mazza, "A biphasic multilayer computational model of human skin," *Biomech Model Mechanobiol*, vol. 20, no. 3, pp. 969–982, 2021, doi: 10.1007/s10237-021-01424-w.

[16] S. Marlar, H. H. Jensen, F. H. Login, and L. N. Nejsum, "Aquaporin-3 in cancer," *International Journal of Molecular Sciences*, vol. 18, no. 10, pp. 1-12, 2017. doi: 10.3390/ijms18102106.

[17] G. Osorio *et al.*, "Expression Pattern of Aquaporin 1 and Aquaporin 3 in Melanocytic and Nonmelanocytic Skin Tumors," *Am J Clin Pathol*, vol. 152, no. 4, pp. 446–457, 2019, doi: 10.1093/ajcp/aqz066.

[18] M. Hara-Chikuma and A. S. Verkman, "Prevention of Skin Tumorigenesis and Impairment of Epidermal Cell Proliferation by Targeted Aquaporin-3 Gene Disruption," *Mol Cell Biol*, vol. 28, no. 1, pp. 326–332, 2008, doi: 10.1128/mcb.01482-07.

[19] G. Tamma *et al.*, "Aquaporin membrane channels in oxidative stress, cell signaling, and aging: Recent advances and research trends," *Oxidative Medicine and Cellular Longevity*, vol. 2018, pp. 1-14, 2018. doi: 10.1155/2018/1501847.

[20] H. Sies, "Hydrogen peroxide as a central redox signaling molecule in physiological oxidative stress: Oxidative eustress," *Redox Biology*, vol. 11, pp. 613–619, 2017. doi: 10.1016/j.redox.2016.12.035.

[21] J. O. Pinho, M. Matias, and M. M. Gaspar, "Emergent nanotechnological strategies for systemic chemotherapy against melanoma," *Nanomaterials*, vol. 9, no. 10, pp. 1-35, 2019. doi: 10.3390/nano9101455.

[22] J. Wang *et al.*, "Aquaporins as diagnostic and therapeutic targets in cancer: How far we are?," *Journal of Translational Medicine*, vol. 13, no. 1, pp. 1-11 2015. doi: 10.1186/s12967-015-0439-7.

[23] T. Gonen and T. Walz, "The structure of aquaporins," *Quarterly Reviews of Biophysics*, vol. 39, no. 4. pp. 361–396, 2006. doi: 10.1017/S0033583506004458.

[24] M. M. Salman, P. Kitchen, A. J. Yool, and R. M. Bill, "Recent breakthroughs and future directions in drugging aquaporins," *Trends in Pharmacological Sciences*, vol. 43, no. 1, pp. 30–42, 2022. doi: 10.1016/j.tips.2021.10.009.

[25] A. P. Martins *et al.*, "Targeting aquaporin function: Potent inhibition of aquaglyceroporin-3 by a gold-based compound," *PLoS One*, vol. 7, no. 5, p.e37435, 2012, doi: 10.1371/journal.pone.0037435.

[26] M. N. Wenzel *et al.*, "Insights into the Mechanisms of Aquaporin-3 Inhibition by Gold(III) Complexes: The Importance of Non-Coordinative Adduct Formation," *Inorg Chem*, vol. 58, no. 3, pp. 2140–2148, 2019, doi: 10.1021/acs.inorgchem.8b03233.

[27] H. D. VanGuilder, K. E. Vrana, and W. M. Freeman, "Twenty-five years of quantitative PCR for gene expression analysis," *BioTechniques*, vol. 44, no. 5. pp. 619–626, 2008. doi: 10.2144/000112776.

[28] E. Grela, J. Kozłowska, and A. Grabowiecka, "Current methodology of MTT assay in bacteria – A review," *Acta Histochemica*, vol. 120, no. 4, pp. 303–311, 2018. doi: 10.1016/j.acthis.2018.03.007.

[29] R. J. Gonzalez and J. B. Tarloff, "Evaluation of hepatic subcellular fractions for Alamar blue and MTT reductase activity.", vol. 15, pp. 257-259, 2001

[30] J. Uggeri *et al.*, "Calcein-AM is a detector of intracellular oxidative activity," *Histochem Cell Biol*, vol. 122, no. 5, pp. 499–505, 2000, doi: 10.1007/s00418-004-0712-y.

[31] SYNENTEC GmnH, "Testing the Toxicity of Calcein-AM under Fluorescence Activated Single Cell Cloning (FASCC) Conditions, "www.synentec.com"

[32] A. Madeira, M. Camps, A. Zorzano, T. F. Moura, and G. Soveral, "Biophysical assessment of human aquaporin-7 as a water and glycerol channel in 3T3-L1 adipocytes," *PLoS One*, vol. 8, no. 12, p. e83442, 2013, doi: 10.1371/journal.pone.0083442.

[33] P. Kumar, A. Nagarajan, and P. D. Uchil, "Analysis of cell viability by the lactate dehydrogenase assay," *Cold Spring Harb Protoc*, vol. 2018, no. 6, pp. 465–468, 2018, doi: 10.1101/pdb.prot095497.

[34] Roche, "Cytotoxicity Detection Kit^{PLUS} (LDH)", version 07, pp. 1-24, 2016, "sigma-aldrich.com."

[35] L. Gao *et al.*, "Aquaporins mediate the chemoresistance of human melanoma cells to arsenite," *Mol Oncol*, vol. 6, no. 1, pp. 81–87, 2012, doi: 10.1016/j.molonc.2011.11.001.

[36] H. Qin, X. Zheng, X. Zhong, A. K. Shetty, P. M. Elias, and W. B. Bollag, "Aquaporin-3 in keratinocytes and skin: Its role and interaction with phospholipase D2," *Archives of Biochemistry and Biophysics*, vol. 508, no. 2. pp. 138–143, 2011. doi: 10.1016/j.abb.2011.01.014.

[37] W. B. Bollag, L. Aitkens, J. White, X. Kelly, and A. Hyndman, "Aquaporin-3 in the epidermis: more than skin deep," *Am J Physiol Cell Physiol*, vol. 318, pp. 1144–1153, 2020, doi: 10.1152/ajpcell.00075.2020.-The.

[38] G. Hendriks *et al.*, "Glycosylation Is Important for Cell Surface Expression of the Water Channel Aquaporin-2 but Is Not Essential for Tetramerization in the Endoplasmic Reticulum," *Journal of Biological Chemistry*, vol. 279, no. 4, pp. 2975–2983, 2004, doi: 10.1074/jbc.M310767200.

[39] C. D. Soares *et al.*, "Comparative expression of cyclooxygenase 2 and ki67 in amelanotic and conventional oral melanoma," *Med Oral Patol Oral Cir Bucal*, vol. 25, no. 6, pp. e728–e731, 2020, doi: 10.4317/medoral.23737.

[40] C. Pimpão *et al.*, "Mechanisms of irreversible aquaporin-10 inhibition by organogold compounds studied by combined biophysical methods and atomistic simulations," *Metallomics*, vol. 13, no. 9, Sep. 2021, doi: 10.1093/mtomcs/mfab053.

[41] C. Pimpão *et al.*, "The aquaporin-3-inhibiting potential of polyoxotungstates," *Int J Mol Sci*, vol. 21, no. 7, pp. 1-11, 2020, doi: 10.3390/ijms21072467.

[42] P. M. Silva *et al.*, "Aquaporin-3 and Aquaporin-5 Facilitate Migration and Cell-Cell Adhesion in Pancreatic Cancer by Modulating Cell Biomechanical Properties," *Cells*, vol. 11, no. 8, pp. 1-17, 2022, doi: 10.3390/cells11081308.

[43] Y. Medina *et al.*, "Lactic Acid Transport Mediated by Aquaporin-9: Implications on the Pathophysiology of Preeclampsia," *Front Physiol*, vol. 12, pp. 1-12, 2021, doi: 10.3389/fphys.2021.774095.

7 Attachments

7.1 Attachment 1 – Western blot reagents

Running buffer (4x): 12 g of Tris base, 57.6 g glycine, and dH_2O until a total of 1 L of solution.

Tris 1.5M pH 8.8: 90.8 g of Tris Base and 300 mL of dH_2O were added and the pH was measured and adjusted with HCl 12 N to 8.8. Then, dH_2O was added until a final volume of 1 L and the solution was autoclaved.

Tris 0.5 M pH 6.8: 6.1 g of Tris Base and 60 mL of dH_2O were added and the pH was measured and adjusted with HCl 12 N to 6.8. Then, dH_2O was added until a final volume of 1 L and the solution was autoclaved.

Transfer buffer: 3.04 g of Tris base (25 mM), 14.4 g glycine (192 mM), 200 mL of methanol (20%), and dH_2O until a total of 1 L of solution.

TBS 10x: 78.8 g of Tris base, 87.66 g of NaCl and 300 mL of dH_2O were added and the pH was measured and adjusted to 7.5. Then, dH_2O was added until a final volume of 1 L.

TBS 1x: 100 mL of TBS, 1 mL of Tween20 and dH_2O until a total of 1 L of solution.

7.2 Gold inhibitors chemical properties

Table 7.1: Summary of the chemical properties of the gold compounds $C^{CO}N$, $C^{NH}N$ and $C^{CH2}N$.

Reference	Weight (mg)	Molecular Weight ($gmol^{-1}$)	Structure
$C^{CO}N$	6.2	450.07	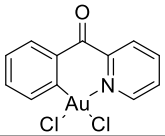
$C^{NH}N$	6.7	437.07	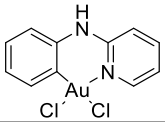
$C^{CH2}N$	7.4	436.09	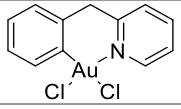

7.3 Attachment 2 – Buffer solutions used in the cell measurements and permeability to water and glycerol assays

For these assays were used three different buffers: HEPES (4-(2-hydroxyethyl)-1-piperazineethanesulfonic acid) 300 mOsm, HEPES 300 mOsm with mannitol (∧=2) 300 mM and HEPES 300 mOsm with glycerol (∧=2) 300 mM. First, 1 L of HEPES 10x was prepared by mixing:

- 78.89 g NaCl
- 3.72 g KCl
- 2.78 g $CaCl_2$
- 2.96 g $MgSO_4$
- 18.02 g D-glucose
- 11.92 g HEPES

After weighting all the components, they were dissolved in distilled water in a 1 L shot. From the HEPES 10x buffer, it was prepared a HEPES 1x buffer by diluting 300 mL of the first one in 2700 mL of distilled water, ending with a 3L solution of HEPES 300 mOsm. The mannitol buffer needed to perform the permeability to water assay was prepared by dissolving 16.392 g of mannitol in 100 mL of HEPES 300 mOsm. Finally, by dissolving 11.056 g of glycerol in 150 mL of HEPES 300 mOsm, the glycerol buffer was obtained.

7.4 Attachment 3 - Cell measurements results

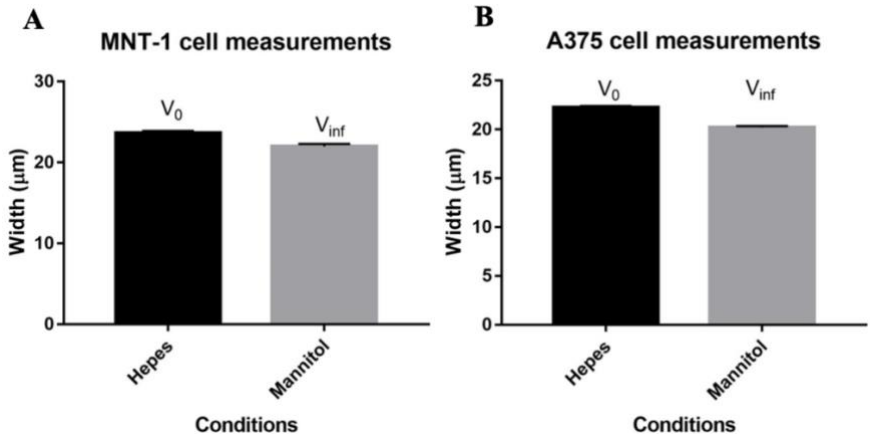

Figure 7.1: Cell measurements performed on MNT-1 and A375 cells**. A-** The measurements performed in the presence of HEPES 300 mOsm were used to obtain the diameter needed for the calculation of the initial volume (V_0) of the cells. **B-** The measurements performed in the presence of HEPES 300 mOsm with Manitol 300 mM were used to obtain the diameter needed for the calculation of the final volume (V_{inf}) of the cells. Data represent means ± SEM of one independent experiment.